Chapter 5
Linear Transversely Isotropic Biphasic Model for Articular Cartilage Layer

Abstract In Sect. 5.1, we develop a linear biphasic theory for the case of a transversely isotropic elastic solid matrix with transverse isotropy of permeability. In Sects. 5.2 and 5.3, we consider the linear biphasic models of confined and unconfined compression, respectively, for the biphasic stress relaxation and the biphasic creep tests. Finally, in Sect. 5.4 we outline the biphasic poroviscoelastic model, which accounts for the inherent viscoelasticity of the solid matrix.

5.1 Linear Biphasic Model

In this section we introduce the linear biphasic theory, which models articular cartilage as a binary mixture of an intrinsically incompressible elastic matrix (skeleton) and an inviscid (i.e., dissipationless) incompressible fluid. We also present and discuss the formulation of the governing differential equations along with the different types of boundary conditions.

5.1.1 Linear Biphasic Theory

According to the biphasic theory of Mow et al. [60], articular cartilage is modeled as a biphasic mixture consisting of a solid phase (representing collagen, proteoglycans, chrondrocytes, and other quantitatively minor glycoproteins) and a fluid phase (representing mobile interstitial fluid and dissolved electrolytes). The fluid phase typically ranges between 65 and 90 % of the articular cartilage tissue by weight [8].

Note also that various biphasic and poroelastic models were used to describe the deformation behavior of bone [20], skin [62], polymeric and silk hydrogels [16, 42], and arterial walls [40]. An overview of computational models for the mechanical behavior of articular cartilage was given in [27, 49, 76].

Let the fluid volume fraction (porosity) be denoted by $\phi_{\mathrm{f}} = V_{\mathrm{f}}/V$, and the solid volume fraction be $\phi_{\mathrm{s}} = V_{\mathrm{s}}/V$, where $V_{\mathrm{f}} + V_{\mathrm{s}} = V$, so that

I. Argatov and G. Mishuris, *Contact Mechanics of Articular Cartilage Layers*,
Advanced Structured Materials 50, DOI 10.1007/978-3-319-20083-5_5

$$\phi_{\mathrm{f}} + \phi_{\mathrm{s}} = 1. \tag{5.1}$$

The continuity equation for a biphasic medium is

$$\nabla \cdot (\phi_{\mathrm{f}} \mathbf{v}^{\mathrm{f}} + \phi_{\mathrm{s}} \mathbf{v}^{\mathrm{s}}) = 0, \tag{5.2}$$

where $\mathbf{v}^{\mathrm{f}}$ and $\mathbf{v}^{\mathrm{s}}$ are solid and fluid velocities, ∇ is the gradient operator.

Under quasi-static conditions, and in the absence of body forces, the momentum equations for each phase are given by

$$\begin{aligned} \nabla \cdot \boldsymbol{\sigma}^{\mathrm{s}} - \boldsymbol{\pi}^{\mathrm{f}} &= \mathbf{0}, \\ \nabla \cdot \boldsymbol{\sigma}^{\mathrm{f}} + \boldsymbol{\pi}^{\mathrm{f}} &= \mathbf{0}, \end{aligned} \tag{5.3}$$

where $\boldsymbol{\pi}^{\mathrm{f}}$ is the momentum exchange between the phases due to frictional drag of relative fluid flow through the porous-permeable solid matrix. In articular cartilage, it has been shown [35] that this momentum exchange term creates a frictional drag several orders of magnitude greater than the viscous shear stress within the interstitial fluid due to the viscosity of the fluid. The internal fluid viscosity can usually be neglected except for very small layers of very permeable materials [11].

Thus, neglecting the frictional dissipation between the fluid particles, the interstitial water is assumed to be inviscid, and the fluid phase stress is given by

$$\boldsymbol{\sigma}^{\mathrm{f}} = -\phi_{\mathrm{f}} p \mathbf{I}. \tag{5.4}$$

Here, p is the fluid pressure, $\mathbf{I}$ is the identity tensor.

The single pore-fluid flow is governed by the local interaction force per unit volume defined as follows [12, 55, 65]:

$$\boldsymbol{\pi}^{\mathrm{f}} = -\mathbf{K} \cdot (\mathbf{v}^{\mathrm{f}} - \mathbf{v}^{\mathrm{s}}). \tag{5.5}$$

Here, $\mathbf{K}$ represents a hydraulic resistivity (or inverse permeability) tensor, which is related to the permeability tensor, $\mathbf{k}$, through

$$\mathbf{K} = \phi_{\mathrm{f}}^2 \mathbf{k}^{-1}, \tag{5.6}$$

and apparently depends on the deformable pore structure and the interstitial fluid properties [58, 59, 67]. Note also that the permeability of the tissue decreases when the pore volume decreases [24, 33].

Generally, $\mathbf{k}$ is a positive definite and symmetric tensor. For a transversely isotropic skeleton, if $x_3 = 0$ is the plane of isotropy, the matrix of the permeability tensor takes the form

$$\mathbf{k} = \begin{pmatrix} k_1 & 0 & 0 \\ 0 & k_1 & 0 \\ 0 & 0 & k_3 \end{pmatrix}.$$

As was shown in [25], the transverse isotropy of permeability in articular cartilage is caused by its microstructural anisotropy. In particular, the permeability is greater in the direction parallel to the collagen fibres than the orthogonal.

In the isotropic case [44], $\mathbf{K} = K\mathbf{I}$, where K is the diffusion coefficient and is related to the permeability coefficient of the solid matrix, k, by $k = \phi_{\mathrm{f}}^2/K$.

The stress-strain relation for the solid matrix is assumed to have the form

$$\boldsymbol{\sigma}^{\mathrm{s}} = -\phi_{\mathrm{s}} p\mathbf{I} + \boldsymbol{\sigma}^{\mathrm{e}}, \tag{5.7}$$

where $\boldsymbol{\sigma}^{\mathrm{e}}$ is the effective (or elastic) stress of the solid matrix. Note that the concept of effective stress was originally formulated by Terzaghi [74] in a geotechnical consolidation problem, presuming that the effective soil stress is determined by the total stress minus the excess pore pressure.

Thus, under these assumptions the total stress in the biphasic material, which is defined as the sum

$$\boldsymbol{\sigma} = \boldsymbol{\sigma}^{\mathrm{s}} + \boldsymbol{\sigma}^{\mathrm{f}}, \tag{5.8}$$

in light of (5.4) and (5.7) is given by

$$\boldsymbol{\sigma} = -p\mathbf{I} + \boldsymbol{\sigma}^{\mathrm{e}}, \tag{5.9}$$

while from (5.3) it follows that

$$\nabla \cdot \boldsymbol{\sigma} = \mathbf{0}. \tag{5.10}$$

For an anisotropic linearly elastic material, the effective stress $\boldsymbol{\sigma}^{\mathrm{e}}$ is related to the infinitesimal strain tensor of the solid matrix, $\boldsymbol{\varepsilon}$, by Hooke's law

$$\boldsymbol{\sigma}^{\mathrm{e}} = \mathbf{C} : \boldsymbol{\varepsilon},$$

where $\mathbf{C}$ is a fourth-order stiffness tensor, and the strain tensor is given by

$$\boldsymbol{\varepsilon} = \frac{1}{2}\left(\nabla\mathbf{u} + \nabla\mathbf{u}^{\mathsf{T}}\right), \tag{5.11}$$

where $\mathbf{u}$ is the displacement vector of the solid phase. Note also that the solid velocity is

$$\mathbf{v}^{\mathrm{s}} = \frac{\partial \mathbf{u}}{\partial t}, \tag{5.12}$$

where t is a time variable.

Following Cohen et al. [19], we assume that the solid-phase material is transversely isotropic, so that

$$\begin{pmatrix} \sigma^{\mathrm{e}}_{11} \\ \sigma^{\mathrm{e}}_{22} \\ \sigma^{\mathrm{e}}_{33} \\ \sigma^{\mathrm{e}}_{23} \\ \sigma^{\mathrm{e}}_{13} \\ \sigma^{\mathrm{e}}_{12} \end{pmatrix} = \begin{bmatrix} A^{\mathrm{s}}_{11} & A^{\mathrm{s}}_{12} & A^{\mathrm{s}}_{13} & 0 & 0 & 0 \\ A^{\mathrm{s}}_{12} & A^{\mathrm{s}}_{11} & A^{\mathrm{s}}_{13} & 0 & 0 & 0 \\ A^{\mathrm{s}}_{13} & A^{\mathrm{s}}_{13} & A^{\mathrm{s}}_{33} & 0 & 0 & 0 \\ 0 & 0 & 0 & 2A^{\mathrm{s}}_{44} & 0 & 0 \\ 0 & 0 & 0 & 0 & 2A^{\mathrm{s}}_{44} & 0 \\ 0 & 0 & 0 & 0 & 0 & 2A^{\mathrm{s}}_{66} \end{bmatrix} \begin{pmatrix} \varepsilon_{11} \\ \varepsilon_{22} \\ \varepsilon_{33} \\ \varepsilon_{23} \\ \varepsilon_{13} \\ \varepsilon_{12} \end{pmatrix}, \tag{5.13}$$

where A^{s}_{11}, A^{s}_{12}, A^{s}_{13}, A^{s}_{33}, and A^{s}_{44} are five independent elastic constants of the solid skeleton.

The substitution of (5.4), (5.5), and (5.7) into Eq. (5.3) yields

$$-\phi_{\mathrm{s}} \nabla p + \nabla \cdot \boldsymbol{\sigma}^{\mathrm{e}} + \mathbf{K} \cdot (\mathbf{v}^{\mathrm{f}} - \mathbf{v}^{\mathrm{s}}) = \mathbf{0}, \tag{5.14}$$

$$-\phi_{\mathrm{f}} \nabla p - \mathbf{K} \cdot (\mathbf{v}^{\mathrm{f}} - \mathbf{v}^{\mathrm{s}}) = \mathbf{0}, \tag{5.15}$$

whereas the substitution of (5.9) into Eq. (5.10) gives

$$-\nabla p + \nabla \cdot \boldsymbol{\sigma}^{\mathrm{e}} = \mathbf{0}. \tag{5.16}$$

Observe [55] that in the equations above, the vector $\mathbf{v}^{\mathrm{f}} - \mathbf{v}^{\mathrm{s}}$ represents the seepage velocity, describing the fluid motion relative to the deforming solid matrix. Moreover, relating this vector only to the fluid part of the mixture, the so-called relative fluid flux (or filter velocity), $\mathbf{w}^{\mathrm{f}}$, can be defined by the formula

$$\mathbf{w}^{\mathrm{f}} = \phi_{\mathrm{f}} (\mathbf{v}^{\mathrm{f}} - \mathbf{v}^{\mathrm{s}}). \tag{5.17}$$

Then, introducing the relative fluid flux into Eq. (5.15) according to its definition (5.17) and taking into account the relation (5.6) between the hydraulic resistivity tensor $\mathbf{K}$ and the permeability tensor $\mathbf{k}$, we arrive at the equation

$$\mathbf{w}^{\mathrm{f}} = -\mathbf{k} \cdot \nabla p, \tag{5.18}$$

which can be interpreted [10] as Darcy's law relative to the motion of the solid matrix.

As a result of (5.1) and (5.17), the continuity equation (5.2) can be recast as

$$\nabla \cdot (\mathbf{v}^{\mathrm{s}} + \mathbf{w}^{\mathrm{f}}) = 0,$$

which after the substitution of (5.12) and (5.18) is reduced to the equation

$$\frac{\partial}{\partial t} \nabla \cdot \mathbf{u} = \nabla \cdot (\mathbf{k} \cdot \nabla p), \tag{5.19}$$

where $\nabla \cdot \mathbf{u}$ is the dilatation of the solid matrix. It is important to note that Eqs. (5.16) and (5.19) can be solved independently of Eq. (5.18).

Observe [19] that the linear transversely isotropic biphasic model requires altogether seven constitutional parameters: five elastic constants (Young's moduli and Poisson's ratios in the transverse plane and out-of-plane, E_1^s, ν_{12}^s and E_3^s, ν_{31}^s, respectively, and the out-of-plane shear modulus, G_{13}^s) and two permeability coefficients k_1 and k_3, which are called the axial (in-plane) and transverse (out-of-plane) permeability coefficients, respectively.

Finally, it should be emphasized [57] that in addition to its mechanical response, articular cartilage also exhibits complex electrochemical phenomena due to the charged nature of its solid phase and the electrolytes dissolved in the interstitial water. A number of constitutive theories [31, 37, 45] for charged-hydrated soft tissues like articular cartilage have been developed using the multiphasic approach (see comprehensive review by Mow and Guo [57]), and a generalized correspondence principle for the equilibrium deformational behavior in the framework of the triphasic model was introduced [52, 53].

5.1.2 Boundary and Initial Conditions

Following Barry and Holmes [10], we consider the most common boundary conditions applicable to thin fluid-saturated porous layers. We assume that a biphasic layer is firmly attached to a rigid impermeable substrate, on the bottom of the layer, $x_3 = h$, in which case the boundary conditions become

$$\mathbf{u}\big|_{x_3=h} = \mathbf{0}, \tag{5.20}$$

$$\left.\frac{\partial p}{\partial x_3}\right|_{x_3=h} = 0. \tag{5.21}$$

On the upper surface, $x_3 = 0$, a number of different boundary conditions may be formulated depending on the problem setting. If the porous layer is in contact with a porous filter, then the boundary condition

$$p\big|_{x_3=0} = 0 \tag{5.22}$$

is imposed on the top surface.

If the layer is pressed against an impermeable punch, then

$$\left.\frac{\partial p}{\partial x_3}\right|_{x_3=0} = 0. \tag{5.23}$$

Further, the normal stress balance under a rigid punch $\sigma_{33}\big|_{x_3=0} = -q$ gives

$$-p + A^{\mathrm{s}}_{13}\frac{\partial u_1}{\partial x_1} + A^{\mathrm{s}}_{13}\frac{\partial u_2}{\partial x_2} + A^{\mathrm{s}}_{33}\frac{\partial u_3}{\partial x_3}\bigg|_{x_3=0} = -q, \tag{5.24}$$

where q is the load distribution on the top surface transferred by the punch. Note that the left-hand side of Eq. (5.24) represents the normal total stress σ_{33}.

For the frictionless contact, the tangential stresses σ_{31} and σ_{32} are zero, so that

$$\frac{\partial u_1}{\partial x_3} + \frac{\partial u_3}{\partial x_1}\bigg|_{x_3=0} = 0, \quad \frac{\partial u_2}{\partial x_3} + \frac{\partial u_3}{\partial x_2}\bigg|_{x_3=0} = 0. \tag{5.25}$$

In an idealized situation, the normal load q would be a known function of variables t, x_1, x_2. However, if the surface load is transferred from a punch, then within the contact area, ω, the contact condition is formulated as

$$u_3\big|_{x_3=0} = \delta_0(t) - \varphi(x_1, x_2), \quad (x_1, x_2) \in \omega, \tag{5.26}$$

where $\delta_0(t)$ is the normal displacement of the punch, $\varphi(x_1, x_2)$ is the punch shape function (defining the initial gap between the contacting surfaces).

Before continuing, we observe that the punch equilibrium implies that

$$\iint_{\omega} q(t, \mathbf{y})\, d\mathbf{y} = F(t), \tag{5.27}$$

where $F(t)$ is an applied external force.

In the case of frictionless contact between two biphasic layers, based on the results of Hou et al. [35] for porous layers saturated with inviscid interstitial fluids, Ateshian et al. [6] formulated the following interface boundary conditions:

$$[\![p]\!] = 0, \quad [\![\mathbf{u}\cdot\mathbf{n}]\!] = \mathbf{0}, \quad [\![\mathbf{w}^{\mathrm{f}}\cdot\mathbf{n}]\!] = \mathbf{0}, \quad [\![\sigma_N^{(n)}]\!] = 0, \tag{5.28}$$

$$\boldsymbol{\sigma}_T^{(n)} = 0. \tag{5.29}$$

Here, $\mathbf{n}$ is the normal unit vector on the contact interface, $[\![\cdot]\!]$ denotes the jump across the interface of the quantity within the brackets (e.g., $[\![p]\!] = p_+ - p_-$, where p_+ and p_- are the limit values of p at the two opposite sides of the interface), $\sigma_N^{(n)}$ and $\boldsymbol{\sigma}_T^{(n)}$ are the normal and tangential components of the total stress vector $\boldsymbol{\sigma}^{(n)} = \boldsymbol{\sigma}\cdot\mathbf{n}$, such that $\sigma_N^{(n)} = \boldsymbol{\sigma}^{(n)}\cdot\mathbf{n}$ and $\boldsymbol{\sigma}_T^{(n)} = \boldsymbol{\sigma}^{(n)} - \sigma_N^{(n)}\mathbf{n}$.

Note that the interface boundary conditions (5.28) simply state that the fluid pressure, p, the normal component of the solid displacement vector, $\mathbf{u}\cdot\mathbf{n}$, the normal component of the relative fluid flow, $\mathbf{w}^{\mathrm{f}}\cdot\mathbf{n}$, and the normal component of the total stress vector, $\sigma_N^{(n)}$, must be continuous across the interface.

Finally, we consider the usual initial conditions that the displacement vector, $\mathbf{u}$, the relative fluid flux, $\mathbf{w}^{\mathrm{f}}$, and the fluid pressure, p, are zero before the external load is applied, i.e.,

$$\mathbf{u} = \mathbf{0}, \quad \mathbf{w}^{\mathrm{f}} = \mathbf{0}, \quad p = 0, \quad -\infty < t < 0, \tag{5.30}$$

throughout the biphasic medium.

5.1.3 *Equivalent Elastic Material Properties of a Transversely Isotropic Biphasic Material for the Instantaneous Response*

It is known [23] that during short-duration impact events, articular cartilage can be considered as an elastic material. Moreover, it has been shown that the instantaneous response of a biphasic material is equivalent to that of an incompressible elastic material [5–7]. Following Garcia et al. [29], we introduce the elastic properties of the equivalent transversely isotropic incompressible elastic material, which can be used to model its instantaneous response.

In the biphasic model (see Eq. (5.8)), the total stresses in a biphasic material are defined as

$$\sigma_{ij} = \sigma_{ij}^{\mathrm{s}} + \sigma_{ij}^{\mathrm{f}}, \tag{5.31}$$

where σ_{ij}^{s} are the stresses in the solid matrix, σ_{ij}^{f} are the stresses in the fluid phase.

The stresses in the fluid phase are equal to the pressure in the fluid, p, averaged over the whole volume, i.e.,

$$\sigma_{ij}^{\mathrm{f}} = -\phi_{\mathrm{f}}\, p\delta_{ij}, \tag{5.32}$$

where ϕ_{f} is the volume fraction of the fluid phase, δ_{ij} is the Kroneker delta.

At the same time, the stresses in the solid matrix are determined in terms of the effective stresses, σ_{ij}^{e}, as

$$\sigma_{ij}^{\mathrm{s}} = -\phi_{\mathrm{s}}\, p\delta_{ij} + \sigma_{ij}^{\mathrm{e}}, \tag{5.33}$$

where $\phi_{\mathrm{s}} = 1 - \phi_{\mathrm{f}}$ is the volume fraction of the solid phase.

From (5.31)–(5.33), it follows that the total stresses in the biphasic tissue can be decomposed as

$$\sigma_{ij} = -p\delta_{ij} + \sigma_{ij}^{\mathrm{e}}. \tag{5.34}$$

It should be emphasized that, since both the fluid and the material forming the skeleton are assumed to be incompressible, the strains in the biphasic tissue are due to the effective stresses. Thus, the strains in the tissue are given by

$$\begin{aligned}
\varepsilon_{11} &= \frac{1}{E_1^{\mathrm{s}}}(\sigma_{11}^{\mathrm{e}} - \nu_{12}^{\mathrm{s}}\sigma_{22}^{\mathrm{e}}) - \frac{\nu_{31}^{\mathrm{s}}}{E_3^{\mathrm{s}}}\sigma_{33}^{\mathrm{e}}, & \varepsilon_{23} &= \frac{1}{2G_{13}^{\mathrm{s}}}\sigma_{23}^{\mathrm{e}},\\
\varepsilon_{22} &= \frac{1}{E_1^{\mathrm{s}}}(-\nu_{12}^{\mathrm{s}}\sigma_{11}^{\mathrm{e}} + \sigma_{22}^{\mathrm{e}}) - \frac{\nu_{31}^{\mathrm{s}}}{E_3^{\mathrm{s}}}\sigma_{33}^{\mathrm{e}}, & \varepsilon_{13} &= \frac{1}{2G_{13}^{\mathrm{s}}}\sigma_{13}^{\mathrm{e}},\\
\varepsilon_{33} &= -\frac{\nu_{31}^{\mathrm{s}}}{E_3^{\mathrm{s}}}(\sigma_{11}^{\mathrm{e}} + \sigma_{22}^{\mathrm{e}}) + \frac{1}{E_3^{\mathrm{s}}}\sigma_{33}^{\mathrm{e}}, & \varepsilon_{12} &= \frac{1}{2G_{12}^{\mathrm{s}}}\sigma_{12}^{\mathrm{e}},
\end{aligned} \tag{5.35}$$

where E_1^{s} and E_3^{s} are Young's moduli of the solid matrix in the plane of transverse isotropy and in the orthogonal direction, respectively, ν_{12}^{s} and ν_{31}^{s} are Poisson's ratios characterizing the lateral strain response in the plane of transverse isotropy to a stress acting parallel or normal to it, respectively, G_{13}^{s} is the shear modulus in planes normal to the plane of transverse isotropy, and $G_{12}^{\mathrm{s}} = E_1^{\mathrm{s}}/[2(1+\nu_{12}^{\mathrm{s}})]$ is the in-plane shear modulus.

For a transversely isotropic material, the incompressibility condition is attained if its Poisson's ratios are as follows [29, 39]:

$$\nu_{31} = \frac{1}{2}, \quad \nu_{12} = 1 - \frac{E_1}{2E_3}. \tag{5.36}$$

Let the three independent constants of the equivalent incompressible elastic material be denoted by E_1, E_3, and G_{13}, while its Poisson's ratios are given by (5.36).

Observe [7] that upon sudden loading of a biphasic tissue, the interstitial fluid does not have sufficient time to leave the tissue, except at permeable boundaries. At time $t = 0^+$, the matrix pores change shape but not volume. Thus, it is assumed [29] that the general stress field in a transversely isotropic biphasic material at time zero can be decomposed into the pressure in the fluid and the effective stresses in the solid skeleton according to Eq. (5.34), in such a way that the fluid pressure at time zero is

$$p = -\alpha\sigma_{kk}. \tag{5.37}$$

Here, $\sigma_{kk} = \sigma_{11} + \sigma_{22} + \sigma_{33}$ is the trace of the total stress tensor, and α is a dimensionless parameter, to be determined.

Thus, on one hand, the deformation of a biphasic material at time zero is given by Eq. (5.35), where in light of the hypothesis (5.37) we have

$$\sigma_{ij}^{\mathrm{e}} = \sigma_{ij} - \alpha\sigma_{kk}\delta_{ij}. \tag{5.38}$$

On the other hand, the same deformation must be equal to the deformation of the equivalent incompressible tissue under the total stress field σ_{ij}. This means, first, that the shear moduli G_{12}^{s} and G_{13}^{s} should be the same for the solid skeleton and the equivalent incompressible elastic material, and in particular,

$$G_{13} = G_{13}^{\mathrm{s}}, \tag{5.39}$$

since the inviscid interstitial fluid sustains only pressure.

Therefore, applying the decomposition (5.38) to normal stresses, one arrives at a homogeneous system of linear algebraic equations with respect to σ_{11}, σ_{22}, and σ_{33}, with the coefficients depending on E_1, E_3, and α. As was shown in [29], this system is satisfied for any combination of the normal stresses, if the equivalent elastic moduli are given by

$$\begin{aligned} E_1 &= \frac{E_1^{\mathrm{s}}\left[1-4\nu_{31}^{\mathrm{s}}+2(1-\nu_{12}^{\mathrm{s}})(E_3^{\mathrm{s}}/E_1^{\mathrm{s}})\right]}{1+\left(1-\nu_{12}^{\mathrm{s}2}\right)(E_3^{\mathrm{s}}/E_1^{\mathrm{s}})-2\nu_{31}^{\mathrm{s}}(1+\nu_{12}^{\mathrm{s}})-\nu_{31}^{\mathrm{s}2}(E_1^{\mathrm{s}}/E_3^{\mathrm{s}})}, \\ E_3 &= \frac{E_3^{\mathrm{s}}\left[1-4\nu_{31}^{\mathrm{s}}+2(1-\nu_{12}^{\mathrm{s}})(E_3^{\mathrm{s}}/E_1^{\mathrm{s}})\right]}{2(1-\nu_{12}^{\mathrm{s}})(E_3^{\mathrm{s}}/E_1^{\mathrm{s}})-4\nu_{31}^{\mathrm{s}2}}. \end{aligned} \tag{5.40}$$

Note that the corresponding decomposition parameter α depends on the applied stresses σ_{11}, σ_{22}, and σ_{33}.

Thus, the instantaneous response of any transversely isotropic biphasic tissue is equivalent to that of an incompressible transversely isotropic elastic material with the material constants ν_{12}, ν_{31}, G_{13}, E_1, and E_3, given by (5.36), (5.39), and (5.40).

We note that in the isotropic case, the equivalent elastic material will also be isotropic, with Poisson's ratio $\nu = 0.5$ and the shear modulus $G = G_{\mathrm{s}}$, where G_{s} is the shear modulus of the elastic skeleton. As a consequence of the relations $E_1^{\mathrm{s}} = E_3^{\mathrm{s}} = 2(1+\nu_{\mathrm{s}})G_{\mathrm{s}}$ and $\nu_{12}^{\mathrm{s}} = \nu_{31}^{\mathrm{s}} = \nu_{\mathrm{s}}$, Eq. (5.40) yield the same result $E_1 = E_3 = 3G_{\mathrm{s}}$, irrespective of the value of the Poisson's ratio ν_{s} of the skeleton.

Note also that if the elastic constants of the elastic skeleton satisfy the incompressibility condition (5.36), then Eq. (5.40) give $E_1 = E_1^{\mathrm{s}}$ and $E_3 = E_3^{\mathrm{s}}$, respectively, when successively taking the limits $\nu_{31}^{\mathrm{s}} \to 0.5$ (with ν_{12}^{s} fixed) and after that as $\nu_{12}^{\mathrm{s}} \to 1 - E_1^{\mathrm{s}}/(2E_3^{\mathrm{s}})$, and vice-versa.

5.1.4 Axisymmetric Biphasic Model

Let us consider a biphasic material with the axis of symmetry oriented along the z axis of an (r, θ, z) cylindrical coordinate system. The constitutive equations (5.13) for the effective stresses of the solid matrix are as follows:

$$\begin{aligned} \sigma_{rr}^{\mathrm{e}} &= A_{11}^{\mathrm{s}}\varepsilon_{rr} + A_{12}^{\mathrm{s}}\varepsilon_{\theta\theta} + A_{13}^{\mathrm{s}}\varepsilon_{zz}, \\ \sigma_{\theta\theta}^{\mathrm{e}} &= A_{12}^{\mathrm{s}}\varepsilon_{rr} + A_{11}^{\mathrm{s}}\varepsilon_{\theta\theta} + A_{13}^{\mathrm{s}}\varepsilon_{zz}, \\ \sigma_{zz}^{\mathrm{e}} &= A_{13}^{\mathrm{s}}\varepsilon_{rr} + A_{13}^{\mathrm{s}}\varepsilon_{\theta\theta} + A_{33}^{\mathrm{s}}\varepsilon_{zz}, \\ \sigma_{rz}^{\mathrm{e}} &= 2A_{44}^{\mathrm{s}}\varepsilon_{rz}. \end{aligned} \tag{5.41}$$

The strain-displacement relations (5.11) become

$$\varepsilon_{rr} = \frac{\partial u_r}{\partial r}, \quad \varepsilon_{\theta\theta} = \frac{u_r}{r}, \quad \varepsilon_{zz} = \frac{\partial u_z}{\partial z}, \quad \varepsilon_{rz} = \frac{1}{2}\Big(\frac{\partial u_r}{\partial z} + \frac{\partial u_z}{\partial r}\Big), \tag{5.42}$$

where u_r and u_z denote the radial and axial displacements.

The equilibrium equations (5.10), which are written with respect to the total stress

$$\boldsymbol{\sigma} = -p\mathbf{I} + \boldsymbol{\sigma}^{\mathrm{e}},$$

now reduce to the following equations of equilibrium:

$$\begin{aligned} -\frac{\partial p}{\partial r} + \frac{1}{r}\frac{\partial (r\sigma^{\mathrm{e}}_{rr})}{\partial r} - \frac{\sigma^{\mathrm{e}}_{\theta\theta}}{r} + \frac{\partial \sigma^{\mathrm{e}}_{rz}}{\partial z} = 0, \\ -\frac{\partial p}{\partial z} + \frac{1}{r}\frac{\partial (r\sigma^{\mathrm{e}}_{rz})}{\partial r} + \frac{\partial \sigma^{\mathrm{e}}_{zz}}{\partial z} = 0. \end{aligned} \tag{5.43}$$

Correspondingly, Eq. (5.19) takes the form

$$\frac{\partial}{\partial t}\left(\frac{\partial u_r}{\partial r} + \frac{u_r}{r} + \frac{\partial u_z}{\partial z}\right) = \frac{1}{r}\frac{\partial}{\partial r}\Big(rk_1\frac{\partial p}{\partial r}\Big) + \frac{\partial}{\partial z}\Big(k_3\frac{\partial p}{\partial z}\Big), \tag{5.44}$$

where k_1 and k_3 are the in-plane and out-of-plane permeability coefficients, while the relative fluid flux can be expressed as

$$\mathbf{w}^{\mathrm{f}} = -k_1\frac{\partial p}{\partial r}\mathbf{e}_r - k_3\frac{\partial p}{\partial z}\mathbf{e}_z, \tag{5.45}$$

with the radial and axial unit coordinate vectors $\mathbf{e}_r$ and $\mathbf{e}_z$, respectively.

5.2 Confined Compression of a Biphasic Material

In this section, we outline a linear confined compression biphasic model. In particular, the biphasic stress relaxation and the biphasic creep tests in confined compression are considered.

5.2.1 Confined Compression Problem

In the confined compression test, a cylindrical plug of biphasic material is constrained in a confining chamber with impermeable rigid walls, and is subjected to a compressive load, $F(t)$, via a porous loading plate (see Fig. 5.1). Observe that the non-linear confined compression problem has been considered in a number of publications [8, 9, 62].

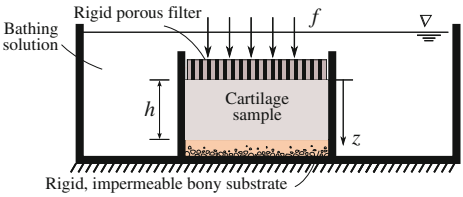

Fig. 5.1 Schematic of the confined compression configuration [52]

In the cylindrical coordinate system, the boundary conditions on the lateral surface are

$$w_r^{\mathrm{f}}\big|_{r=a} = 0, \quad \sigma_{rz}\big|_{r=a} = \sigma_{r\theta}\big|_{r=a} = 0, \quad u_r\big|_{r=a} = 0, \tag{5.46}$$

where w_r^{f} is the transverse (in-plane) relative fluid flux, σ_{rz} and $\sigma_{r\theta}$ are out-of-plane and in-plane total shear stresses, and u_r is the radial displacement of the solid matrix.

The boundary conditions at the bottom surface, $z = h$, are as follows:

$$w_z^{\mathrm{f}}\big|_{z=h} = 0, \quad \sigma_{zr}\big|_{z=h} = \sigma_{z\theta}\big|_{z=h} = 0. \quad u_z\big|_{z=h} = 0, \tag{5.47}$$

Here, w_z^{f} and u_z are the vertical relative fluid flux and the vertical displacement of the solid matrix, respectively.

Meanwhile, the boundary conditions at the top surface, $z = 0$, have the form

$$p\big|_{z=0} = 0, \quad \sigma_{zr}\big|_{z=0} = \sigma_{z\theta}\big|_{z=0} = 0, \tag{5.48}$$

where p is the interstitial fluid pressure.

Observe that the boundary condition $(5.48)_1$ describes the free-draining porous interface, where no resistance to fluid movement is assumed at the interface between the porous loading plate and the sample surface.

For the stress relaxation test, the additional boundary condition at the top is

$$u_z\big|_{z=0} = w(t), \tag{5.49}$$

where $w(t)$ is a specified displacement of the loading plate.

For example, the ramp displacement is defined as

$$w(t) = \begin{cases} V_0 t, & 0 \le t \le t_0, \\ V_0 t_0, & t_0 \le t, \end{cases} \tag{5.50}$$

and V_0, t_0 are given constants.

On the other hand, for creep, the boundary condition is

$$\sigma_{zz}\big|_{z=0} = -\frac{F(t)}{A}, \tag{5.51}$$

where $F(t)$ is a specified external load acting on the porous loading plate, and $A = \pi a^2$ is the sample cross-sectional area.

For example, if the load is applied instantaneously, then

$$F(t) = F_0 \mathscr{H}(t), \tag{5.52}$$

where $\mathscr{H}(t)$ is the Heaviside step function.

The experimental setup of the confined compression test for articular cartilage represents a one-dimensional problem in the axial direction, so that

$$u_r = u_\theta = 0, \quad \varepsilon_{rr} = \varepsilon_{\theta\theta} = 0, \quad w_r^{\mathrm{f}} = w_\theta^{\mathrm{f}} = 0, \tag{5.53}$$

while all non-trivial variables are dependent on t and z only.

Note that the assumptions $(5.53)_1$ and $(5.53)_2$ dictate that the rigid confining chamber prevents any lateral deformation. Therefore, the axial total stress is

$$\sigma_{zz} = -p + H_A \varepsilon_{zz}, \tag{5.54}$$

where H_A is the confined compression equilibrium modulus (aggregate elastic modulus) of the solid matrix given by

$$H_A = A_{33}^{\mathrm{s}}. \tag{5.55}$$

Hence, taking into account the free-draining condition $(5.48)_1$, the traction boundary condition (5.51) can be reduced to the following:

$$H_A \frac{\partial u_z}{\partial z}\Big|_{z=0} = -f(t). \tag{5.56}$$

Here, $f(t)$ is the applied compressive stress, i.e.,

$$f(t) = \frac{F(t)}{A}. \tag{5.57}$$

Finally, to complete the confined compression problem formulation, we assume the usual initial conditions (5.30).

5.2.2 Governing Equation of the Confined Compression Model

Under the assumptions made in the confined compression model, the only equilibrium differential equation $(5.43)_2$ takes the form

$$-\frac{\partial p}{\partial z}+\frac{\partial \sigma_{zz}^{\mathrm{e}}}{\partial z}=0, \tag{5.58}$$

where, in light of (5.53) and (5.54), we have

$$\sigma_{zz}^{\mathrm{e}}=H_A\varepsilon_{zz}. \tag{5.59}$$

Integrating Eq. (5.59) with respect to the coordinate z, we arrive at the equation

$$-p+\sigma_{zz}^{\mathrm{e}}=\sigma_{zz}(t). \tag{5.60}$$

Here, $\sigma_{zz}(t)$ is the integration constant (being a function of the time variable t only).

Now, comparing Eqs. (5.54) and (5.60), we find that the total normal stress, $\sigma_{zz}(t)$, is uniform through the depth of the biphasic sample.

Further, since all non-trivial variables are dependent on t and z only, the equilibrium equation (5.44) for the fluid phase after integration with respect to the coordinate z reduces to

$$\frac{\partial u_z}{\partial t}=k_3\frac{\partial p}{\partial z}, \tag{5.61}$$

where k_3 is the axial permeability coefficient.

Now, collecting Eqs. (5.59)–(5.61), we arrive at the governing equation

$$\frac{\partial u_z}{\partial t}=k_3\frac{\partial}{\partial z}\left(H_A\frac{\partial u_z}{\partial z}\right), \tag{5.62}$$

which for a homogeneous biphasic material simplifies to a Fourier equation

$$\frac{\partial u_z}{\partial t}=k_3H_A\frac{\partial^2 u_z}{\partial z^2}. \tag{5.63}$$

Equation (5.63) is supplemented by the homogeneous initial condition

$$u_z(0,z)=0$$

and the boundary condition at the bottom surface

$$u_z(t,h)=0.$$

For stress relaxation, the general boundary condition at the top surface is

$$u_z(t,0)=w(t), \tag{5.64}$$

where $w(t)$ is the prescribed surface displacement as a function of time, while for creep, in light of (5.56), we have

$$\frac{\partial u_z}{\partial z}(t,0) = -\frac{f(t)}{H_A}, \tag{5.65}$$

where $f(t)$ is the prescribed compressive stress as a function of time.

Note that the second-order parabolic partial differential equation (5.62) was solved in [26] using a semi-analytical approach based on the finite difference and Laplace transform methods. The effect of the depth-dependent aggregate modulus on articular cartilage stress-relaxation in confined compression was studied in [75].

5.2.3 Biphasic Stress Relaxation in Confined Compression

The following formula [64] gives the general solution to the problem (5.63) and (5.64):

$$u_z(t,z) = w(t)\left(1-\frac{z}{h}\right) - \sum_{n=1}^{\infty} \frac{2}{\pi n} \sin\left(\pi n \frac{z}{h}\right)\left(\mathscr{K}_n w\right)(t). \tag{5.66}$$

Here we have introduced the notation

$$\left(\mathscr{K}_n w\right)(t) = \int_{0^-}^{t} \exp\left(-\frac{n^2(t-\tau)}{\tau_R'}\right)\dot{w}(\tau)\,d\tau, \tag{5.67}$$

where τ_R' is the characteristic relaxation time in confined compression defined by

$$\tau_R' = \frac{h^2}{\pi^2 k_3 H_A}. \tag{5.68}$$

Recall that the lower integration limit 0^- in the integral operator above indicates that the integration in (5.67) starts at infinitesimally negative time so as to include the displacement discontinuity at time zero.

The strain of the solid matrix can be simply obtained from the relationship

$$\varepsilon_{zz} = \frac{\partial u_z}{\partial z}.$$

Then according to Eq. (5.60), we have

$$p = H_A \varepsilon_{zz} - \sigma_{zz}(t), \tag{5.69}$$

from which we can determine the total normal stress, in light of the free-draining boundary condition $(5.48)_1$, as follows:

$$\sigma_{zz}(t) = H_A \varepsilon_{zz}\big|_{z=0}.$$

The interstitial hydrostatic pressure can be expressed in the form

$$p(t,z) = \frac{2H_A}{h}\sum_{n=1}^{\infty}\Big[1-\cos\Big(\pi n\frac{z}{h}\Big)\Big]\big(\mathscr{K}_n w\big)(t). \tag{5.70}$$

The corresponding stress relaxation response in confined compression is then given by

$$\sigma_{zz}(t) = -H_A\frac{w(t)}{h} - \frac{2H_A}{h}\sum_{n=1}^{\infty}\big(\mathscr{K}_n w\big)(t). \tag{5.71}$$

In the case of constant strain rate compression in the loading phase $t \in (0, t_0)$, followed by the hold period $t \in (t_0, +\infty)$, formula (5.50) yields

$$\dot{w}(t) = \begin{cases} V_0, & 0 \le t \le t_0, \\ 0, & t_0 \le t. \end{cases}$$

Therefore, in the case of ramp displacement (5.50), the integral (5.67), which appears on the right-hand sides of (5.66), (5.70), and (5.71), is evaluated as

$$\begin{aligned} \big(\mathscr{K}_n w\big)(t) &= \frac{V_0\tau_R'}{n^2}\Big(1-\exp\Big(-\frac{n^2 t}{\tau_R'}\Big)\Big), \quad 0 \le t < t_0, \\ \big(\mathscr{K}_n w\big)(t) &= \frac{V_0\tau_R'}{n^2}\exp\Big(-\frac{n^2 t}{\tau_R'}\Big)\Big(\exp\Big(\frac{n^2 t_0}{\tau_R'}\Big)-1\Big), \quad t_0 \le t. \end{aligned}$$

Now, taking into account the above formulas and the identity

$$\sum_{n=1}^{\infty}\frac{1}{n^2} = \frac{\pi^2}{6},$$

we arrive at the following formulas [60]:

$$\sigma_{zz}(t) = -H_A\frac{V_0 t}{h} - \frac{V_0 h}{3k_3} + \frac{2V_0 h}{\pi^2 k_3}\sum_{n=1}^{\infty}\frac{1}{n^2}\exp\Big(-\frac{n^2 t}{\tau_R'}\Big) \tag{5.72}$$

for $0 \le t < t_0$, and

$$\sigma_{zz}(t) = -H_A\frac{V_0 t_0}{h} + \frac{2V_0 h}{\pi^2 k_3}\sum_{n=1}^{\infty}\frac{1}{n^2}\left\{\exp\Big(-\frac{n^2 t}{\tau_R'}\Big) - \exp\Big(-\frac{n^2(t-t_0)}{\tau_R'}\Big)\right\} \tag{5.73}$$

for $t \ge t_0$.

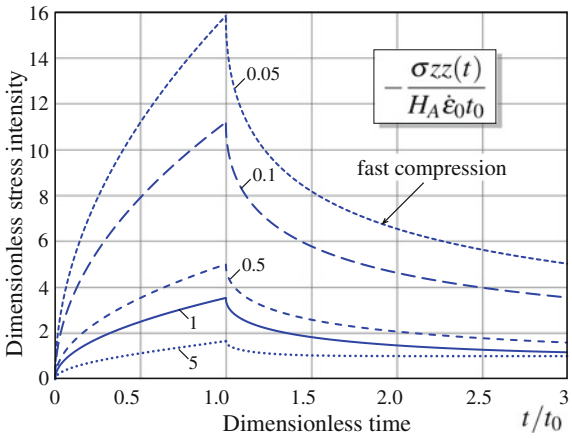

Fig. 5.2 The effect of t_0/τ_R' on the stress-relaxation time history in response to a ramped displacement. (The values taken by t_0/τ_R' are indicated on the figure.) Note the limit value 1 as $t \to \infty$ in all cases due to the normalization

According to Eqs. (5.72) and (5.73), the effect of t_0/τ_R' on the dimensionless stress-relaxation time history $-\sigma_{zz}(t)/[H_A \dot{\varepsilon}_0 t_0]$, where $\dot{\varepsilon}_0 = V_0/h$, is shown in Fig. 5.2.

Equations (5.72) and (5.73) can be used for determining the aggregate modulus, H_A, and the constant axial permeability coefficient, k_3, from the stress relaxation experiment by fitting the theoretical solution on to the experimental curve for the measured total normal stress [69].

5.2.4 Biphasic Creep in Confined Compression

The following formula [64] gives the general solution to the problem (5.63) and (5.65):

$$u_z(t,z) = \frac{2k_3}{h} \sum_{n=1}^{\infty} \cos\left(\frac{\pi(2n-1)z}{2h}\right) \left(\mathcal{N}_n f\right)(t). \tag{5.74}$$

Here we have introduced the notation

$$\left(\mathcal{N}_n f\right)(t) = \int_0^t \exp\left(-(2n-1)^2 \frac{(t-\tau)}{\tau_R''}\right) f(\tau)\, d\tau, \tag{5.75}$$

where τ_R' is the characteristic time having the meaning of a retardation time in confined compression defined as

$$\tau_R'' = \frac{4h^2}{\pi^2 k_3 H_A}. \tag{5.76}$$

Thus, the nominal sample-average strain (surface-to-surface strain), which is calculated from the distance $h - u_z(t,0)$ between the loading platens, is

$$\frac{u_z(t,0)}{h} = \frac{2k_3}{h^2}\sum_{n=1}^{\infty}\big(\mathscr{N}_n f\big)(t). \tag{5.77}$$

Taking into account the constitutive equation (5.60) and the boundary conditions $(5.48)_1$ and (5.56), we find that the total normal stress in the biphasic sample is

$$\sigma_{zz}(t) = -f(t).$$

Hence, Eq. (5.69) allows evaluation of the interstitial hydrostatic pressure via

$$p = H_A\varepsilon_{zz} + f(t). \tag{5.78}$$

Evaluating the strain of the solid matrix according to formula (5.74) and substituting the obtained result into Eq. (5.78), we find

$$p(t,z) = f(t) - \frac{\pi k_3 H_A}{h^2}\sum_{n=1}^{\infty}(2n-1)\sin\Big(\frac{\pi(2n-1)z}{2h}\Big)\big(\mathscr{N}_n f\big)(t). \tag{5.79}$$

For a creep experiment, where a constant external load, F_0, is applied instantaneously, the following loading law holds true (see Eq. (5.57)):

$$f(t) = f_0\mathscr{H}(t). \tag{5.80}$$

Here, $\mathscr{H}(t)$ is the Heaviside step function, $f_0 = F_0/A$ is the constant compressive stress, and A is the cross-sectional area of the biphasic sample.

Correspondingly, formula (5.77) yields the following result [14]:

$$\frac{u_z(t,0)}{h} = \frac{f_0}{H_A}\left\{1 - \frac{8}{\pi^2}\sum_{n=1}^{\infty}\frac{1}{(2n-1)^2}\exp\Big(-(2n-1)^2\frac{t}{\tau_R''}\Big)\right\}. \tag{5.81}$$

Note that in writing (5.81), we used the identity

$$\sum_{n=1}^{\infty}\frac{1}{(2n-1)^2} = \frac{\pi^2}{8}.$$

In the same way, in the case (5.80), formula (5.79) is rearranged to obtain

$$p(t,z) = \frac{4f_0}{\pi}\sum_{n=1}^{\infty}\frac{1}{2n-1}\sin\Big(\frac{\pi(2n-1)z}{2h}\Big)\exp\Big(-(2n-1)^2\frac{t}{\tau_R''}\Big). \tag{5.82}$$

In writing (5.82), the following identity was used (see, e.g., [30], formula (1.442.1)):

$$\sum_{n=1}^{\infty} \frac{\sin(2n-1)\zeta}{2n-1} = \frac{\pi}{4}, \quad 0 < \zeta < \pi. \tag{5.83}$$

By substituting $z = h$ into Eq. (5.82), we readily obtain

$$p(t,h) = \frac{4f_0}{\pi} \sum_{k=0}^{\infty} \frac{(-1)^k}{2k+1} \exp\left(-(2k+1)^2 \frac{t}{\tau_R''}\right). \tag{5.84}$$

Note also [69] that the interstitial fluid pressure at the impermeable interface, $z = h$, can be represented by the formula

$$p(t,h) = H_A\left(\varepsilon_{zz}\big|_{z=h} - \varepsilon_{zz}\big|_{z=0}\right),$$

where ε_{zz} is the strain of the solid matrix, $\varepsilon_{zz} = \partial u_z/\partial z$, while the displacement u_z is taken from (5.74) for creep and from (5.66) for stress relaxation.

Correspondingly, the so-called fluid load support

$$\frac{W^p}{W} = \frac{p(t,h)}{f(t)}$$

is evaluated as follows [63]:

$$\frac{W^p}{W} = \left(\frac{\partial u}{\partial z}\Big|_{z=0} - \frac{\partial u}{\partial z}\Big|_{z=h}\right) \Big/ \frac{\partial u}{\partial z}\Big|_{z=0}.$$

In the stepwise creep test, according to (5.80) and (5.84), we have

$$\frac{W^p}{W} = \frac{4}{\pi} \sum_{k=0}^{\infty} \frac{(-1)^k}{2k+1} \exp\left(-(2k+1)^2 \frac{t}{\tau_R''}\right).$$

Therefore, as a consequence of (5.83), the above formula yields the maximum value

$$\frac{W^p}{W}\Big|_{t=0} = 1.$$

It should be noted [63] that in real creep testing configurations, there exists a delay in pressurization due to the impedance of the pressure transducer in measuring the pressure $p(t,h)$. Namely, the greater the compliance of the pressure transducer, the greater the delay in the interstitial fluid pressurization achieving the peak value of W^p/W.

Equation (5.81) is commonly used in determining the aggregate modulus, H_A, and the constant axial permeability coefficient, k_3, from the confined compression creep experiment by fitting the theoretical solution on to the experimental curve for the nominal sample-average strain. It should be mentioned that for improved mechanical characterization of articular cartilage, testing experiments may involve multiple-step ramp loading [50] as well as an alternating sequence of stress relaxation and creep transients [17].

Finally, observe [13] that the presence of a gap between the loading plate and the confining chamber walls, which is necessary to guarantee a correct plate movement, allows flow exudation and tissue extrusion around the plate, thus leading to underestimation of H_A and overestimation of k_3.

5.2.5 *Dynamic Behavior of a Biphasic Material Under Cyclic Compressive Loading in Confined Compression*

Let us now consider the following loading history for cyclic compressive confined compression [70, 73]:

$$f(t) = f_0(1 - \cos \omega t)\mathscr{H}(t). \tag{5.85}$$

Here, f_0 is the median magnitude of the applied cyclic stress, and ω is the loading angular frequency. Recall that $\omega/(2\pi)$ is the loading frequency measured in hertz.

First of all, using integration by parts and the identity (see, e.g., [30], formula (1.444.6))

$$\sum_{n=1}^{\infty} \frac{\cos(2n-1)\zeta}{(2n-1)^2} = \frac{\pi}{4}\Big(\frac{\pi}{2} - \zeta\Big), \quad 0 < \zeta < \pi,$$

we transform formulas (5.74) and (5.79) as follows:

$$u_z(t,z) = \frac{h}{H_A}\Big\{ f(t)\Big(1 - \frac{z}{h}\Big) - \frac{8}{\pi^2}\sum_{n=1}^{\infty} \frac{1}{(2n-1)^2} \cos\Big(\frac{\pi(2n-1)z}{2h}\Big)\big(\mathscr{M}_n f\big)(t)\Big\}, \tag{5.86}$$

$$p(t,z) = \frac{4}{\pi}\sum_{n=1}^{\infty} \frac{1}{2n-1} \sin\Big(\frac{\pi(2n-1)z}{2h}\Big)\big(\mathscr{M}_n f\big)(t). \tag{5.87}$$

Here we have introduced the notation

$$\big(\mathscr{M}_n f\big)(t) = \int_{0^-}^{t} \exp\Big(-(2n-1)^2 \frac{(t-\tau)}{\tau_R''}\Big) \dot{f}(\tau)\, d\tau. \tag{5.88}$$

As usual, the notation 0^- in the lower limit of the integral above means that

$$\int_{0^-}^{t} e^{-a_n(t-\tau)}\dot{f}(\tau)\,d\tau = f(0^+)e^{-a_n t} + \int_{0}^{t} e^{-a_n(t-\tau)}\dot{f}(\tau)\,d\tau,$$

where $f(0^+)$ is the limit of the function $f(t)$ when the independent variable t approaches 0 from the right.

Since $f(0) = 0$ for the function defined by formula (5.85), we have

$$\dot{f}(\tau) = \omega f_0 \mathscr{H}(t)\sin\omega t,$$

so that Eqs. (5.86) and (5.87) yield

$$\begin{aligned} u_z(t,z) = \frac{f_0 h}{H_A}\Bigg\{ & (1-\cos\omega t)\Big(1-\frac{z}{h}\Big) \\ & - \frac{8}{\pi^2}\sin\omega t \sum_{n=1}^{\infty} \frac{\omega a_n}{(2n-1)^2(a_n^2+\omega^2)} \cos\Big(\frac{\pi(2n-1)z}{2h}\Big) \\ & + \frac{8}{\pi^2}\cos\omega t \sum_{n=1}^{\infty} \frac{\omega^2}{(2n-1)^2(a_n^2+\omega^2)} \cos\Big(\frac{\pi(2n-1)z}{2h}\Big) \\ & - \frac{8}{\pi^2}\sum_{n=1}^{\infty} \frac{\omega^2}{(2n-1)^2(a_n^2+\omega^2)} \exp(-a_n t)\cos\Big(\frac{\pi(2n-1)z}{2h}\Big)\Bigg\} \end{aligned} \tag{5.89}$$

for the vertical displacement of the solid matrix and

$$\begin{aligned} p(t,z) = \frac{4f_0}{\pi}\Bigg\{ & \sin\omega t \sum_{n=1}^{\infty} \frac{\omega a_n}{(2n-1)(a_n^2+\omega^2)} \sin\Big(\frac{\pi(2n-1)z}{2h}\Big) \\ & - \cos\omega t \sum_{n=1}^{\infty} \frac{\omega^2}{(2n-1)(a_n^2+\omega^2)} \sin\Big(\frac{\pi(2n-1)z}{2h}\Big) \\ & + \sum_{n=1}^{\infty} \frac{\omega^2}{(2n-1)(a_n^2+\omega^2)} \exp(-a_n t)\sin\Big(\frac{\pi(2n-1)z}{2h}\Big)\Bigg\} \end{aligned} \tag{5.90}$$

for the interstitial fluid pressure, where we have introduced the notation

$$a_n = \frac{(2n-1)^2}{\tau_R''}.$$

It can be checked that Eqs. (5.89) and (5.90) coincide with the corresponding results obtained by Suh et al. [73], apart from notation.

5.3 Unconfined Compression of a Biphasic Material

In this section, the unconfined compression biphasic model is developed. In particular, the biphasic stress relaxation and the biphasic creep tests in unconfined compression are studied.

5.3.1 Unconfined Compression Problem

In the axisymmetric unconfined compression test, a thin cylindrical disk of biphasic material is compressed between two smooth (frictionless) and impermeable rigid platens (see Fig. 5.3). Therefore, the material is free to expand radially, and free fluid flow is enabled across the lateral cylindrical surface.

In the cylindrical coordinate system, the boundary conditions on the lateral surface are

$$p\big|_{r=a} = 0, \quad \sigma_{rz}\big|_{r=a} = \sigma_{r\theta}\big|_{r=a} = \sigma_{rr}\big|_{r=a} = 0. \tag{5.91}$$

Here, p is the interstitial fluid pressure, σ_{rz} and $\sigma_{r\theta}$ are shear stresses, σ_{rr} is the radial normal stress.

The boundary conditions at the bottom surface, $z = h$, are

$$w_z^{\mathrm{f}}\big|_{z=h} = 0, \quad \sigma_{zr}\big|_{z=h} = \sigma_{z\theta}\big|_{z=h} = 0, \quad u_z\big|_{z=h} = 0, \tag{5.92}$$

where w_z^{f} and u_z are the vertical relative fluid flux and the vertical displacement of the solid matrix, respectively.

At the top surface, $z = 0$, we have the following boundary conditions:

$$w_z^{\mathrm{f}}\big|_{z=0} = 0, \quad \sigma_{zr}\big|_{z=0} = \sigma_{z\theta}\big|_{z=0} = 0, \quad u_z\big|_{z=0} = w(t). \tag{5.93}$$

Here, $w(t)$ is the vertical displacement of the upper platen.

Again, we can consider either the creep test (load-controlled) or the stress-relaxation test (displacement-controlled) in unconfined compression. For the stress-relaxation experiment, $w(t)$ is a prescribed function of time.

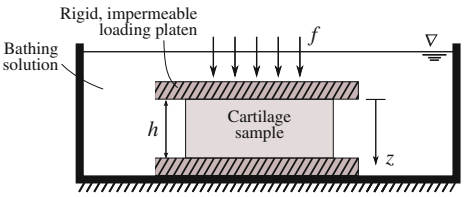

Fig. 5.3 Schematic of the unconfined compression configuration [52]. The articular cartilage sample has to be stripped off from the subchondral bone and cut into a perfect cylinder

Following Armstrong et al. [5] and Cohen et al. [19], we assume the radial displacement of the solid skeleton, u_r, the fluid relative radial velocity, w_r^{f}, and the fluid pressure, p, to be of the form

$$u_r = u_r(t, r), \quad w_r^{\mathrm{f}} = w_r^{\mathrm{f}}(t, r), \quad p = p(t, r). \tag{5.94}$$

Moreover, the axial strain, ε_{zz}, is assumed to be uniform throughout the sample, i.e.,

$$\varepsilon_{zz} = \varepsilon(t), \tag{5.95}$$

where $\varepsilon(t)$ is a time-dependent function.

Hence, in light of the assumption (5.95), the integration of the equation

$$\varepsilon_{zz} = \frac{\partial u_z}{\partial z}$$

with the boundary conditions $(5.92)_3$ and $(5.93)_3$ taken into account yields

$$\varepsilon(t) = -\frac{w(t)}{h}, \tag{5.96}$$

$$u_z(t, z) = -\varepsilon(t)(h - z). \tag{5.97}$$

According to (5.94), (5.95), and (5.97), the only nonzero strain components are

$$\varepsilon_{rr} = \frac{\partial u_r}{\partial r}, \quad \varepsilon_{\theta\theta} = \frac{u_r}{r}, \quad \varepsilon_{zz} = \varepsilon,$$

and, correspondingly, Eq. (5.41) yield the following nonzero effective stresses:

$$\begin{aligned}
\sigma_{rr}^{\mathrm{e}} &= A_{11}^{\mathrm{s}} \frac{\partial u_r}{\partial r} + A_{12}^{\mathrm{s}} \frac{u_r}{r} + A_{13}^{\mathrm{s}} \varepsilon, \\
\sigma_{\theta\theta}^{\mathrm{e}} &= A_{12}^{\mathrm{s}} \frac{\partial u_r}{\partial r} + A_{11}^{\mathrm{s}} \frac{u_r}{r} + A_{13}^{\mathrm{s}} \varepsilon, \\
\sigma_{zz}^{\mathrm{e}} &= A_{13}^{\mathrm{s}} \frac{\partial u_r}{\partial r} + A_{13}^{\mathrm{s}} \frac{u_r}{r} + A_{33}^{\mathrm{s}} \varepsilon.
\end{aligned} \tag{5.98}$$

The substitution of (5.98) into the equilibrium equations for the solid matrix (5.43) results in the differential equation

$$-\frac{\partial p}{\partial r} + A_{11}^{\mathrm{s}} \left(\frac{\partial^2 u_r}{\partial r^2} + \frac{1}{r} \frac{\partial u_r}{\partial r} - \frac{u_r}{r^2} \right) = 0, \tag{5.99}$$

while Eq. (5.44) takes the form

$$\frac{\partial}{\partial t}\left(\frac{\partial u_r}{\partial r}+\frac{u_r}{r}+\varepsilon\right)=\frac{1}{r}\frac{\partial}{\partial r}\left(rk_1\frac{\partial p}{\partial r}\right), \tag{5.100}$$

where k_1 is the transverse (in-plane) permeability coefficient.

Finally, the relative fluid flux (5.45), in light of (5.94), is given by

$$\mathbf{w}^{\mathrm{f}}=-k_1\frac{\partial p}{\partial r}\mathbf{e}_r, \tag{5.101}$$

where $\mathbf{e}_r$ is the radial unit vector.

Equations (5.99)–(5.101), with the boundary conditions (5.91)–(5.93) and the zero initial conditions, constitute the unconfined compression problem.

It has been established [57] that the incorporation of a transverse isotropy for material properties into the linear biphasic theory improves its predictive power in unconfined compression analysis [19].

5.3.2 *Solution of the Unconfined Compression Problem*

Let us first turn to Eq. (5.100). Taking into account that

$$\frac{\partial u_r}{\partial r}+\frac{u_r}{r}=\frac{1}{r}\frac{\partial}{\partial r}(ru_r),$$

we can integrate Eq. (5.100) once with respect to the radial coordinate to get

$$\frac{\partial p}{\partial r}=\frac{1}{k_1}\frac{\partial}{\partial t}\left(u_r+\frac{\varepsilon}{2}r\right), \tag{5.102}$$

where the integration constant vanishes due to the regularity condition at the center of the sample, $r=0$.

Therefore, Eqs. (5.99) and (5.102) yield the following equation [19]:

$$\frac{\partial^2 u_r}{\partial r^2}+\frac{1}{r}\frac{\partial u_r}{\partial r}-\frac{u_r}{r^2}=\frac{1}{A^{\mathrm{s}}_{11}k_1}\frac{\partial}{\partial t}\left(u_r+\frac{\varepsilon}{2}r\right). \tag{5.103}$$

Recall that the boundary conditions $(5.91)_2$ are formulated in terms of the components of the total stress tensor

$$\boldsymbol{\sigma}=-p\mathbf{I}+\boldsymbol{\sigma}^{\mathrm{e}}. \tag{5.104}$$

Hence, as a consequence of the constitutive equation (5.98), the boundary conditions (5.91) become

$$p\big|_{r=a} = 0, \quad A^{\mathrm{s}}_{11}\frac{\partial u_r}{\partial r} + A^{\mathrm{s}}_{12}\frac{u_r}{r} + A^{\mathrm{s}}_{13}\varepsilon\,\Big|_{r=a} = 0. \tag{5.105}$$

To simplify our treatment of the problem, we introduce dimensionless variables

$$\rho = \frac{r}{a}, \quad U = \frac{u_r}{a}, \quad \tau = \frac{A^{\mathrm{s}}_{11}k_1}{a^2}t, \quad P = \frac{p}{A^{\mathrm{s}}_{11}}. \tag{5.106}$$

Then, Eqs. (5.102)–(5.105) take the form

$$\frac{\partial P}{\partial \rho} = \frac{\partial}{\partial \tau}\Big(U + \frac{\varepsilon}{2}\rho\Big), \tag{5.107}$$

$$\frac{\partial^2 U}{\partial \rho^2} + \frac{1}{\rho}\frac{\partial U}{\partial \rho} - \frac{U}{\rho^2} = \frac{\partial}{\partial \tau}\Big(U + \frac{\varepsilon}{2}\rho\Big), \tag{5.108}$$

$$P\big|_{\rho=1} = 0, \quad \frac{\partial U}{\partial \rho} + \alpha_{12}\frac{U}{\rho} + \alpha_{13}\varepsilon\,\Big|_{\rho=1} = 0, \tag{5.109}$$

where we have introduced the notation

$$\alpha_{12} = \frac{A^{\mathrm{s}}_{12}}{A^{\mathrm{s}}_{11}}, \quad \alpha_{13} = \frac{A^{\mathrm{s}}_{13}}{A^{\mathrm{s}}_{11}}. \tag{5.110}$$

Now, let $\tilde{P}(s)$, $\tilde{U}(s)$, and $\tilde{\varepsilon}(s)$ denote the Laplace transforms with respect to the dimensionless time τ. Taking into account the zero initial conditions, the Laplace transformation of Eqs. (5.107)–(5.109) leads to the system

$$\frac{\partial \tilde{P}}{\partial \rho} = s\Big(\tilde{U} + \frac{\tilde{\varepsilon}}{2}\rho\Big), \tag{5.111}$$

$$\frac{\partial^2 \tilde{U}}{\partial \rho^2} + \frac{1}{\rho}\frac{\partial \tilde{U}}{\partial \rho} - \frac{\tilde{U}}{\rho^2} = s\Big(\tilde{U} + \frac{\tilde{\varepsilon}}{2}\rho\Big), \tag{5.112}$$

$$\tilde{P}\big|_{\rho=1} = 0, \quad \frac{\partial \tilde{U}}{\partial \rho} + \alpha_{12}\frac{\tilde{U}}{\rho} + \alpha_{13}\tilde{\varepsilon}\,\Big|_{\rho=1} = 0. \tag{5.113}$$

The general solution of Eq. (5.112) can be represented in the form

$$\tilde{U} = -\frac{\tilde{\varepsilon}}{2}\rho + \tilde{U}_0, \tag{5.114}$$

where $\tilde{U}_0$ is the general solution of the homogeneous equation corresponding to Eq. (5.112), i.e.,

$$\frac{\partial^2 \tilde{U}_0}{\partial \rho^2} + \frac{1}{\rho}\frac{\partial \tilde{U}_0}{\partial \rho} - \left(s + \frac{1}{\rho^2}\right)\tilde{U}_0 = 0. \tag{5.115}$$

Making use of the change of the independent variable $\rho = \rho'/\sqrt{s}$, Eq. (5.115) can be reduced to the modified Bessel's equation. In this way, taking into account the regularity condition at $\rho = 0$, we obtain

$$\tilde{U}_0 = C_0 I_1(\sqrt{s}\rho), \tag{5.116}$$

where C_0 is an arbitrary function of the Laplace transform parameter s. This integration constant (with respect to the variable ρ) should be determined from the boundary condition $(5.113)_2$, which in light of (5.114) becomes

$$\frac{\partial \tilde{U}_0}{\partial \rho} + \alpha_{12}\frac{\tilde{U}_0}{\rho}\bigg|_{\rho=1} = \frac{\tilde{\varepsilon}}{2}(1 + \alpha_{12} - 2\alpha_{13}).$$

By substituting the expression (5.116) into the above equation and taking into account the identity $I_1'(x) = I_0(x) - (1/x)I_1(x)$ for the modified Bessel functions of the first kind, we find

$$C_0 = \frac{(1 + \alpha_{12} - 2\alpha_{13})\tilde{\varepsilon}(s)}{2\left[\sqrt{s}I_0(\sqrt{s}) - (1 - \alpha_{12})I_1(\sqrt{s})\right]}. \tag{5.117}$$

Collecting formulas (5.114)–(5.117), we obtain

$$\tilde{U} = -\frac{\tilde{\varepsilon}}{2}\rho\left(1 - \frac{(1 + \alpha_{12} - 2\alpha_{13})I_1(\sqrt{s}\rho)}{\sqrt{s}\rho\left(I_0(\sqrt{s}) - (1 - \alpha_{12})\dfrac{I_1(\sqrt{s})}{\sqrt{s}}\right)}\right). \tag{5.118}$$

We now calculate the Laplace transform of the dimensionalized pressure, $\tilde{P}$, from Eq. (5.111), which as a result of (5.114) can be rewritten as

$$\frac{\partial \tilde{P}}{\partial \rho} = s\tilde{U}_0.$$

The integration of the above equation with respect to ρ, in light of the identity $I_0'(x) = I_1(x)$, yields

$$\tilde{P} = C_0\sqrt{s}I_0(\sqrt{s}\rho) + C_1,$$

where C_1 is an arbitrary function of s. By satisfying the boundary condition $(5.113)_1$, we immediately get $C_1 = -C_0\sqrt{s}I_0(\sqrt{s})$ and

$$\tilde{P} = C_0\sqrt{s}\left(I_0(\sqrt{s}\rho) - I_0(\sqrt{s})\right), \tag{5.119}$$

where C_0 is given by (5.117).

Finally, we consider the force response of the biphasic sample

$$F(t) = -2\pi \int_0^a \sigma_{zz}(t, r) r \, dr, \tag{5.120}$$

where, in light of (5.98) and (5.104), the out-of-plane normal total stress is given by

$$\sigma_{zz} = -p + A^{\mathrm{s}}_{13} \frac{\partial u_r}{\partial r} + A^{\mathrm{s}}_{13} \frac{u_r}{r} + A^{\mathrm{s}}_{33} \varepsilon. \tag{5.121}$$

In terms of the dimensionless variables (5.106), Eq. (5.120) takes the form

$$\mathscr{F}(\tau) = -2 \int_0^1 \left(-P + \alpha_{13} \left(\frac{\partial U}{\partial \rho} + \frac{U}{\rho} \right) + \alpha_{33} \varepsilon \right) \rho \, d\rho, \tag{5.122}$$

where we have introduced the notation

$$\mathscr{F}(\tau) = \frac{F(t)}{\pi a^2 A^{\mathrm{s}}_{11}}, \tag{5.123}$$

$$\alpha_{33} = \frac{A^{\mathrm{s}}_{33}}{A^{\mathrm{s}}_{11}}. \tag{5.124}$$

After application of the Laplace transform, Eq. (5.122) becomes

$$\tilde{\mathscr{F}}(s) = -2 \int_0^1 \left(-\tilde{P} + \alpha_{13} \left(\frac{\partial \tilde{U}}{\partial \rho} + \frac{\tilde{U}}{\rho} \right) + \alpha_{33} \tilde{\varepsilon} \right) \rho \, d\rho. \tag{5.125}$$

Now, taking into account Eqs. (5.114), (5.117), (5.119) and formulas

$$I_0'(x) = I_1(x), \quad x I_1'(x) = x I_0(x) - I_1(x),$$

the integral (5.125) becomes

$$\tilde{\mathscr{F}}(s) = -\frac{\gamma_1 I_0(\sqrt{s}) - \gamma_2 \dfrac{I_1(\sqrt{s})}{\sqrt{s}}}{I_0(\sqrt{s}) - \gamma_0 \dfrac{I_1(\sqrt{s})}{\sqrt{s}}} \tilde{\varepsilon}(s), \tag{5.126}$$

where we have also introduced the notation

$$\begin{aligned}\gamma_0 &= 1-\alpha_{12},\\ \gamma_1 &= \frac{1}{2}(1+\alpha_{12}+2\alpha_{33}-4\alpha_{13}),\\ \gamma_2 &= \alpha_{33}(1-\alpha_{12})+1+\alpha_{12}-4\alpha_{13}+2\alpha_{13}^2.\end{aligned} \tag{5.127}$$

Formulas (5.126) and (5.127) coincide with the corresponding results given by Cohen et al. [19], up to the notation. In the isotropic case, we have

$$\alpha_{12}=\alpha_{13}=\frac{\lambda_s}{H_A},\quad \alpha_{33}=1,\quad \gamma_0=\frac{2\mu_s}{H_A},\quad \gamma_1=\frac{3\mu_s}{H_A},\quad \gamma_2=\frac{8\mu_s^2}{H_A^2},$$

where λ_s, μ_s, and H_A are the Lamé elastic constants and the aggregate elastic modulus of the solid skeleton, respectively, and the original results of Armstrong et al. [5] are immediately recovered.

5.3.3 Unconfined Compression Model

Following [3], we rewrite Eq. (5.126) in the form

$$\tilde{\mathscr{F}}(s)=-s\tilde{\varepsilon}(s)\tilde{\mathscr{K}}(s), \tag{5.128}$$

where we have introduced the notation

$$\tilde{\mathscr{K}}(s)=\frac{\gamma_1 I_0(\sqrt{s})-\gamma_2\dfrac{I_1(\sqrt{s})}{\sqrt{s}}}{s\left(I_0(\sqrt{s})-\gamma_0\dfrac{I_1(\sqrt{s})}{\sqrt{s}}\right)}. \tag{5.129}$$

By applying the convolution theorem to Eq. (5.128), we obtain

$$\mathscr{F}(\tau)=-\int_{0^-}^{\tau}\frac{d\varepsilon(\tau')}{d\tau'}\mathscr{K}(\tau-\tau')\,d\tau', \tag{5.130}$$

where $\mathscr{K}(\tau)=\mathscr{L}^{-1}\{\tilde{\mathscr{K}}(s)\}$ is the original function of $\tilde{\mathscr{K}}(s)$, and $\tau=0^-$ is the dimensionless time moment just preceding the initial moment of loading $\tau=0$. In deriving Eq. (5.130), we have used the formula

$$\mathscr{L}^{-1}\{s\tilde{\varepsilon}(s)\}=\frac{d\varepsilon(\tau)}{d\tau}+\varepsilon(0^+)\delta(\tau),$$

where $\delta(\tau)$ is the Dirac function.

Following [5], we calculate the inverse Laplace transform by using the residue theorem (see, e.g., [46, 48]) to find

$$\mathscr{K}(\tau) = \frac{2\gamma_1 - \gamma_2}{2 - \gamma_0} + \sum_{n=1}^{\infty} \frac{2(\gamma_2 - \gamma_0\gamma_1)}{\alpha_n^2 - \gamma_0(2 - \gamma_0)} e^{-\alpha_n^2 \tau}, \tag{5.131}$$

where α_n are the roots of the transcendental equation

$$J_0(x) - \gamma_0 \frac{J_1(x)}{x} = 0, \tag{5.132}$$

in which $J_0(x)$ and $J_1(x)$ are Bessel functions of the first kind.

The inverse relation for Eq. (5.130) can be represented by

$$\varepsilon(\tau) = -\int_{0^-}^{\tau} \frac{d\mathscr{F}(\tau')}{d\tau'} \mathscr{M}(\tau - \tau')\, d\tau', \tag{5.133}$$

where $\mathscr{M}(\tau) = \mathscr{L}^{-1}\{\tilde{\mathscr{M}}(s)\}$, and $\tilde{\mathscr{M}}(s)$ is defined by the formula

$$\tilde{\mathscr{M}}(s) = \frac{I_0(\sqrt{s}) - \gamma_0 \dfrac{I_1(\sqrt{s})}{\sqrt{s}}}{s\left(\gamma_1 I_0(\sqrt{s}) - \gamma_2 \dfrac{I_1(\sqrt{s})}{\sqrt{s}}\right)}. \tag{5.134}$$

Again making use of the residue theorem, we obtain

$$\mathscr{M}(\tau) = \frac{2 - \gamma_0}{2\gamma_1 - \gamma_2} - \sum_{n=1}^{\infty} \frac{2(\gamma_2 - \gamma_0\gamma_1)}{\gamma_1^2 \beta_n^2 + \gamma_2(\gamma_2 - 2\gamma_1)} e^{-\beta_n^2 \tau}, \tag{5.135}$$

where β_n are the roots of the transcendental equation

$$J_0(x) - \frac{\gamma_2}{\gamma_1} \frac{J_1(x)}{x} = 0. \tag{5.136}$$

The short-time asymptotic approximation for the kernel $\mathscr{K}(\tau)$, as can also be found for $\mathscr{M}(\tau)$, can be obtained by evaluating the Laplace inverse of $\tilde{\mathscr{K}}(s)$ as $s \to \infty$. For this purpose, we apply the following well known asymptotic expansion (see, e.g., [30], formula (8.451.5)):

$$I_n(z) = \frac{e^z}{\sqrt{2\pi z}} \left\{1 + \frac{(1 - 4n^2)}{8z} + O(z^{-2})\right\}.$$

By making use of the above asymptotic formula, we expand the right-hand sides of (5.129) and (5.134) in terms of $1/\sqrt{s}$. As a result, we arrive at the following asymptotic expansions:

$$\mathscr{K}(\tau) = \gamma_1 - \frac{2}{\sqrt{\pi}}(\gamma_2 - \gamma_0\gamma_1)\sqrt{\tau} + O(\tau), \quad \tau \to 0^+, \tag{5.137}$$

$$\mathscr{M}(\tau) = \frac{1}{\gamma_1} + \frac{2}{\sqrt{\pi}}\frac{(\gamma_2 - \gamma_0\gamma_1)}{\gamma_1^2}\sqrt{\tau} + O(\tau), \quad \tau \to 0^+. \tag{5.138}$$

The asymptotic approximations (5.137) and (5.138) can be used in evaluating unconfined impact compression tests where the impact duration is relatively small compared to the so-called [5] gel diffusion time for the biphasic material $t_{\mathrm{g}} = a^2/(H_A k_1)$, which is the time taken for a cylindrical biphasic sample of radius a to reach equilibrium in unconfined stepwise compression.

Further, let us introduce the notation

$$\mathscr{K}_0 = \mathscr{K}(0), \quad \mathscr{M}_0 = \mathscr{M}(0).$$

In light of (5.137) and (5.138), we have

$$\mathscr{K}_0 = \gamma_1, \quad \mathscr{M}_0 = \frac{1}{\gamma_1}. \tag{5.139}$$

Hence, the following identities hold true:

$$\begin{aligned} \frac{2\gamma_1 - \gamma_2}{2 - \gamma_0} + \sum_{n=1}^{\infty} \frac{2(\gamma_2 - \gamma_0\gamma_1)}{\alpha_n^2 - \gamma_0(2 - \gamma_0)} &= \gamma_1, \\ \frac{2 - \gamma_0}{2\gamma_1 - \gamma_2} - \sum_{n=1}^{\infty} \frac{2(\gamma_2 - \gamma_0\gamma_1)}{\gamma_1^2\beta_n^2 + \gamma_2(\gamma_2 - 2\gamma_1)} &= \frac{1}{\gamma_1}. \end{aligned} \tag{5.140}$$

Using Eq. (5.140), we can rewrite the kernel functions (5.131) and (5.135) as

$$\begin{aligned} \mathscr{K}(\tau) &= \mathscr{K}_0 - \sum_{n=1}^{\infty} \frac{2(\gamma_2 - \gamma_0\gamma_1)}{\alpha_n^2 - \gamma_0(2 - \gamma_0)}\left(1 - e^{-\alpha_n^2\tau}\right), \\ \mathscr{M}(\tau) &= \mathscr{M}_0 + \sum_{n=1}^{\infty} \frac{2(\gamma_2 - \gamma_0\gamma_1)}{\gamma_1^2\beta_n^2 + \gamma_2(\gamma_2 - 2\gamma_1)}\left(1 - e^{-\beta_n^2\tau}\right), \end{aligned} \tag{5.141}$$

and then introduce the normalized kernel functions

$$K(t) = \frac{1}{\mathscr{K}_0}\mathscr{K}\left(\frac{A_{11}^{\mathrm{s}} k_1}{a^2}t\right), \quad M(t) = \frac{1}{\mathscr{M}_0}\mathscr{M}\left(\frac{A_{11}^{\mathrm{s}} k_1}{a^2}t\right), \tag{5.142}$$

so that, in light of (5.106) and (5.139)–(5.142), we have

$$K(t) = 1 - \sum_{n=1}^{\infty} \mathscr{A}_n \left(1 - \exp\left(-\frac{t}{\rho_n}\right)\right), \tag{5.143}$$

$$M(t) = 1 + \sum_{n=1}^{\infty} \mathscr{B}_n \left(1 - \exp\left(-\frac{t}{\tau_n}\right)\right), \tag{5.144}$$

where we have introduced the notation

$$\mathscr{A}_n = \frac{2(\gamma_2 - \gamma_0\gamma_1)}{\gamma_1\left[\alpha_n^2 - \gamma_0(2 - \gamma_0)\right]}, \quad \mathscr{B}_n = \frac{2\gamma_1(\gamma_2 - \gamma_0\gamma_1)}{\gamma_1^2\beta_n^2 + \gamma_2(\gamma_2 - 2\gamma_1)}, \tag{5.145}$$

$$\rho_n = \frac{a^2}{\alpha_n^2 A_{11}^{\mathrm{s}} k_1}, \quad \tau_n = \frac{a^2}{\beta_n^2 A_{11}^{\mathrm{s}} k_1}. \tag{5.146}$$

Note that, by analogy with the viscoelastic model, the functions $K(t)$ and $M(t)$ may be called the normalized biphasic relaxation function and the normalized biphasic creep function for unconfined compression, respectively. Note also that the sequences $\rho_1 > \rho_2 > \ldots$ and $\tau_1 > \tau_2 > \ldots$, which are defined by formulas (5.146), represent the discrete relaxation and retardation spectra, respectively.

In the dimensional form, Eqs. (5.130) and (5.133) can be recast as follows (see formulas (5.96), (5.106), and (5.123)):

$$F(t) = \frac{\pi a^2 E_3}{h} \int_{0^-}^{t} K(t - t')\dot{w}(t')\, dt', \tag{5.147}$$

$$w(t) = \frac{h}{\pi a^2 E_3} \int_{0^-}^{t} M(t - t')\dot{F}(t')\, dt'. \tag{5.148}$$

Here we have introduced the notation

$$E_3 = A_{11}^{\mathrm{s}} \mathscr{K}_0 = \frac{A_{11}^{\mathrm{s}}}{\mathscr{M}_0},$$

which according to Eqs. (5.110), (5.124), (5.127), and (5.139), has the form

$$E_3 = \frac{1}{2}\left(A_{11}^{\mathrm{s}} + A_{12}^{\mathrm{s}} + 2A_{33}^{\mathrm{s}} - 4A_{13}^{\mathrm{s}}\right). \tag{5.149}$$

Note that the elastic constant E_3 defined by formula (5.149) coincides with the out-of-plane Young's modulus of the equivalent (for instantaneous response) transversely isotropic incompressible elastic material given by formula $(5.40)_2$.

In terms of the technical elastic constants, formulas (5.127) yield

$$\gamma_0 = \frac{1 - \nu_{12}^{\mathrm{s}} - 2\nu_{31}^{\mathrm{s}2} n_1}{1 - \nu_{31}^{\mathrm{s}2} n_1}, \tag{5.150}$$

$$\frac{\gamma_2}{\gamma_1} = \frac{2\left\{\left[1 - 4\nu_{31}^{\mathrm{s}}(1 - \nu_{12}^{\mathrm{s}}\nu_{31}^{\mathrm{s}})\right] n_1 + (1 - \nu_{12}^{\mathrm{s}})^2 - \nu_{31}^{\mathrm{s}2}(1 - 4\nu_{31}^{\mathrm{s}}) n_1^2\right\}}{\left(1 - n_1 \nu_{31}^{\mathrm{s}2}\right)\left[(1 - 4\nu_{31}^{\mathrm{s}}) n_1 + 2(1 - \nu_{12}^{\mathrm{s}})\right]}, \tag{5.151}$$

where we have introduced the notation

$$n_1 = \frac{E_1^{\mathrm{s}}}{E_3^{\mathrm{s}}}.$$

Finally, we note that in light of (5.150), Eq. (5.132) coincides with the corresponding equation derived in [19].

5.3.4 Biphasic Stress Relaxation in Unconfined Compression

For an imposed step displacement, i.e.,

$$w(t) = w_0 \mathscr{H}(t),$$

where $\mathscr{H}(t)$ is the Heaviside step function, by formula (5.147) we have

$$F(t) = \pi a^2 E_3 \frac{w_0}{h} K(t), \tag{5.152}$$

for $K(t)$ and E_3 given by (5.143) and (5.149).

Following Cohen et al. [19], we consider the ratio of the peak load intensity (F_{peak}, at $t \to 0^+$) to the one at equilibrium (F_{eq}, at $t \to +\infty$), which in light of the relations $K(0) = 1$ and $K(+\infty) = 1 - \sum_{n=1}^{\infty} \mathscr{A}_n$ takes the form

$$\frac{F_{\mathrm{peak}}}{F_{\mathrm{eq}}} = \frac{\gamma_1(2 - \gamma_0)}{2\gamma_1 - \gamma_2}. \tag{5.153}$$

We note that in writing the above equation we have used the first identity (5.140).

In the isotropic case, the right-hand side of (5.153) reduces to $3/[2(1 + \nu_{\mathrm{s}})]$, which is a strictly decreasing function of Poisson's ratio ν_{s} and for positive ν_{s} attains a maximum value of 1.5 at $\nu_{\mathrm{s}} = 0$, as shown by Armstrong et al. [5].

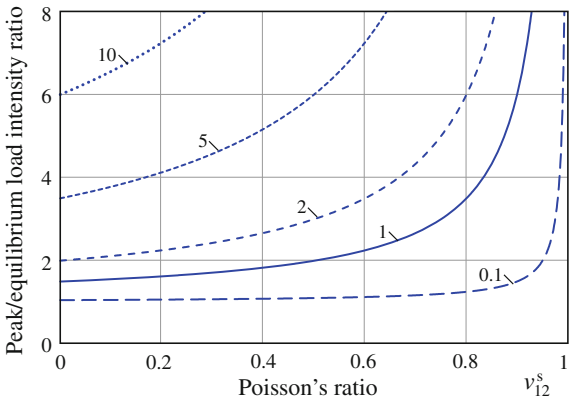

Fig. 5.4 The effect of ν_{12}^{s} and E_1^s/E_3^s on the peak to equilibrium ratio of the load intensity in the stress-relaxation response to a step displacement. (The values taken by E_1^s/E_3^s are indicated on the figure)

Taking into account formulas (5.110), (5.124), and (5.127), we rewrite Eq. (5.153) in the following form [19]:

$$\frac{F_{\text{peak}}}{F_{\text{eq}}} = \frac{2(1-\nu_{12}^{s}) + (1-4\nu_{31}^{s})E_1^s/E_3^s}{2\big(1-\nu_{12}^{s}-2\nu_{31}^{s2}E_1^s/E_3^s\big)}. \tag{5.154}$$

For the particular case of $\nu_{31}^{s} = 0$, the maximum values of the load intensity ratio are depicted in Fig. 5.4 for different values of E_1^s/E_3^s and $\nu_{12}^{s} \in (0, 1.0)$. Note the high values that this ratio can attain (much greater than the maximum value 1.5 for the ratio $F_{\text{peak}}/F_{\text{eq}} = 3/[2(1+\nu)]$ in the isotropic case for $\nu = 0$).

For an imposed ramp displacement, i.e.,

$$w(t) = \begin{cases} V_0 t, & 0 \le t \le t_0, \\ V_0 t_0, & t_0 \le t, \end{cases}$$

when a constant strain rate $-V_0/h$ is maintained until time t_0, the general solution (3.49) yields

$$F(t) = \pi a^2 E_3 \frac{V_0}{h}\left\{\frac{(2\gamma_1-\gamma_2)}{\gamma_1(2-\gamma_0)}t + \sum_{n=1}^{\infty}\mathscr{A}_n\rho_n\big(1-e^{-t/\rho_n}\big)\right\} \tag{5.155}$$

for $0 \le t \le t_0$, and for $t \ge t_0$ gives

$$F(t) = \pi a^2 E_3 \frac{V_0}{h}\left\{\frac{(2\gamma_1-\gamma_2)}{\gamma_1(2-\gamma_0)}t_0 + \sum_{n=1}^{\infty}\mathscr{A}_n\rho_n\big(e^{-(t-t_0)/\rho_n}-e^{-t/\rho_n}\big)\big)\right\}. \tag{5.156}$$

Note that at equilibrium (as $t \to \infty$), the load intensity will be

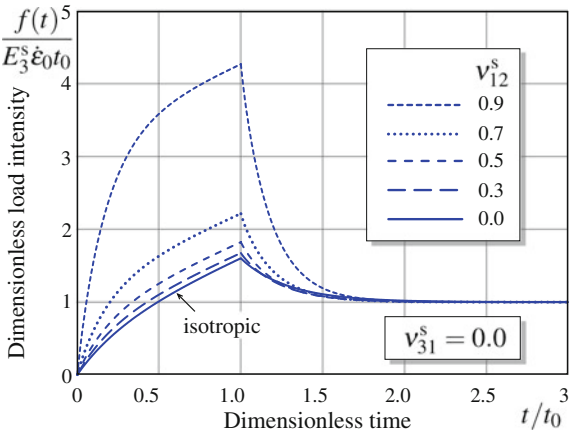

Fig. 5.5 The effect of ν_{12}^s on the stress-relaxation time history in response to a ramped displacement, when $E_1^s/E_3^s = 5$ and $t_0/t_g = 1$

$$F_{eq} = \pi a^2 E_3 \frac{(2\gamma_1 - \gamma_2)}{\gamma_1(2-\gamma_0)} \frac{V_0 t_0}{h},$$

which in light of (5.110), (5.124), and (5.127), reduces to

$$F_{eq} = \pi a^2 E_3^s \frac{V_0 t_0}{h}. \tag{5.157}$$

The characteristic relaxation time in unconfined compression can be defined by

$$\tau_R' = \frac{a^2}{\alpha_1^2 A_{11}^s k_1}, \tag{5.158}$$

where α_1 is the first root of the transcendental equation (5.132).

For the special case in which $\nu_{31}^s = 0$, $E_1^s/E_3^s = 5$, and the ratio of the ramp time to the gel diffusion time, $t_g = a^2/(A_{11}^s k_1)$ (cf. formula (5.158)), is $t_0/t_g = 1$, the effect of ν_{12}^s on the dimensionless stress-relaxation time history $f(t)/[E_3^s \dot{\varepsilon}_0 t_0]$, where $f(t) = F(t)/[\pi a^2]$ and $\dot{\varepsilon}_0 = V_0/h$, is shown in Fig. 5.5. Also, according to Cohen et al. [19], Fig. 5.6 illustrates the effect of the ratio t_0/t_g on the stress relaxation time history for the special case of $\nu_{12}^s = 0.3$, $\nu_{31}^s = 0$, and $E_1^s/E_3^s = 5$.

We also note an alternative representation for $F(t)$ in the loading stage, similar to the one obtained in [19], which follows from the direct inverse Laplace transform of Eq. (5.128) for $\tilde{\varepsilon}(s) = -(V_0 t_g/h)s^{-2}$. Then, for $0 \le t \le t_0$ we have

$$F(t) = \pi a^2 E_3 \frac{V_0}{h} \left\{ \frac{(2\gamma_1 - \gamma_2)}{\gamma_1(2-\gamma_0)} t + \frac{\gamma_2 - \gamma_0\gamma_1}{4\gamma_1(2-\gamma_0)^2} - \sum_{n=1}^{\infty} \mathscr{A}_n \rho_n e^{-t/\rho_n} \right\}.$$

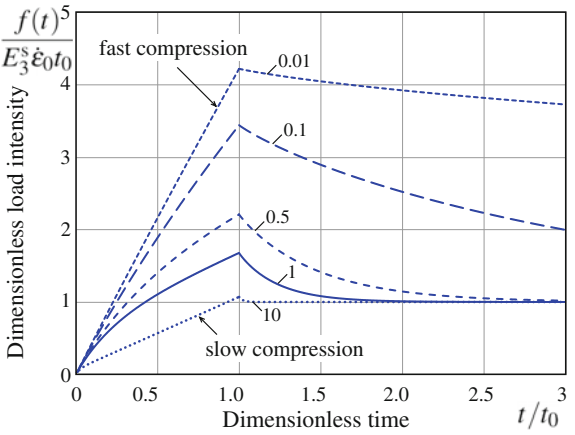

Fig. 5.6 The effect of t_0/t_g on the stress-relaxation time history in response to a ramped displacement, when $\nu_{12}^s = 0.3$, $\nu_{31}^s = 0.0$, and $E_1^s/E_3^s = 5$. (The values taken by t_0/t_g are indicated on the figure)

Equations (5.155) and (5.156) can be used in determining the material properties from the unconfined stress relaxation experiment, by fitting the theoretical solution on to the experimental curve for the total normal stress [19, 32].

5.3.5 *Biphasic Creep in Unconfined Compression*

For an imposed step loading, $F(t) = F_0 \mathscr{H}(t)$, we obtain from formula (5.148) that

$$w(t) = \frac{hF_0}{\pi a^2 E_3} M(t), \tag{5.159}$$

where $M(t)$ and E_3 are given by (5.144) and (5.149).

Taking into account Eqs. $(5.140)_2$ and $(5.145)_2$, we find

$$M(t) = \frac{\gamma_2 + 2\gamma_1^2 - \gamma_1(\gamma_0 + \gamma_2)}{\gamma_1(2\gamma_1 - \gamma_2)} - \sum_{n=1}^{\infty} \mathscr{B}_n \exp\left(-\frac{t}{\tau_n}\right), \tag{5.160}$$

where γ_0, γ_1, γ_2 and $\mathscr{B}_n$, τ_n are given by (5.127) and $(5.145)_2$, $(5.146)_2$, respectively.

The characteristic retardation time in unconfined compression can be defined by

$$\tau_R'' = \frac{a^2}{\beta_1^2 A_{11}^s k_1},$$

where β_1 is the first root of the transcendental equation (5.136).

In the isotropic case, formulas (5.159) and (5.160) reduce to the solution originally obtained by Armstrong et al. [5].

Equations (5.159) and (5.160) are used in determining the biphasic materials properties from the unconfined compression creep experiment by fitting the theoretical solution with the experimental curve for the nominal strain [5, 47].

Observe that the deformation response is characterized by an instantaneous jump

$$w(0^+) = \frac{hF_0}{\pi a^2 E_3}$$

followed by a decreasing slope until equilibrium is reached, where

$$w(+\infty) = \frac{hF_0}{\pi a^2 E_3^{\mathrm{s}}}.$$

Note that the identity

$$E_3 = \frac{\gamma_1(2\gamma_1 - \gamma_2)}{\gamma_2 + 2\gamma_1^2 - \gamma_1(\gamma_0 + \gamma_2)} E_3^{\mathrm{s}}$$

can be directly proved using the expressions (5.110), (5.124), (5.127), and (5.149).

In the isotropic case, when the deformation behavior of the solid phase is described by two elastic constants E_{s} and ν_{s}, the equilibrium response of biphasic material in unconfined and confined compression allows us to evaluate the Young's modulus E_{s} and the aggregate modulus H_A. Thus, taking into account that

$$H_A = \frac{1 - \nu_{\mathrm{s}}}{(1 + \nu_{\mathrm{s}})(1 - 2\nu_{\mathrm{s}})} E_{\mathrm{s}},$$

the following formula for Poisson's ratio can be derived [43]:

$$\nu_{\mathrm{s}} = \frac{1}{4}\left(\frac{E_{\mathrm{s}}}{H_A} - 1 + \sqrt{\left(\frac{E_{\mathrm{s}}}{H_A} - 1\right)\left(\frac{E_{\mathrm{s}}}{H_A} - 9\right)}\right).$$

Finally, note that platen/specimen friction influences the mechanical response of articular cartilage in unconfined compression [5, 71, 77]. In particular, the peak reaction forces in unconfined stress-relaxation experiments exceed the corresponding maximum values predicted analytically. Consequently, the frictional effect becomes more significant for specimens with large aspect (diameter/height) ratios.

5.3.6 Cyclic Compressive Loading in Unconfined Compression

It is well known that the long-term creep and relaxation tests, typically used for determining viscoelastic and biphasic/poroelastic properties, are not appropriate for rapidly assessing the dynamic biomechanical properties of biological tissues like

articular cartilage. For in vivo measurements of tissue viability, Appleyard et al. [1] developed a dynamic indentation instrument, which employs a single-frequency (20 Hz) sinusoidal oscillatory waveform superimposed on a carrier load.

Following Li et al. [51], we assume that a biphasic tissue sample is subjected to a cyclic displacement input

$$w(t) = [w_0(1 - \cos \omega t) + w_1]\mathscr{H}(t), \tag{5.161}$$

where w_1/h is the prestrain resulting from the initial deformation applied to the sample to create the desired preload, w_0 is the displacement amplitude, i.e., w_0/h is equal to one-half the peak-to-peak cyclic strain input superimposed on the prestrain, and $\omega = 2\pi f$ is the angular frequency, f being the loading frequency.

Differentiating (5.161), we obtain

$$\frac{dw(t)}{dt} = \mathscr{H}(t) w_0 \omega \sin \omega t + w_1 \delta(t). \tag{5.162}$$

Substituting expression (5.162) into Eq. (5.147), we arrive, after some algebra, at the following stress output:

$$\frac{F(t)}{\pi a^2} = \frac{E_3}{h}\left\{ w_1 K(t) + w_0 \left(\frac{2\gamma_1 - \gamma_2}{\gamma_1(2 - \gamma_0)} + \sum_{n=1}^{\infty} \frac{\rho_n^2 \omega^2 \mathscr{A}_n}{1 + \rho_n^2 \omega^2} \exp\left(-\frac{t}{\rho_n}\right)\right)\right.$$
$$\left. - w_0\left[K_1(\omega)\cos \omega t - K_2(\omega) \sin \omega t\right]\right\}. \tag{5.163}$$

Here we have introduced the notation

$$K_1(\omega) = 1 - \sum_{n=1}^{\infty} \frac{\mathscr{A}_n}{1 + \rho_n^2 \omega^2}, \tag{5.164}$$

$$K_2(\omega) = \sum_{n=1}^{\infty} \frac{\rho_n \omega \mathscr{A}_n}{1 + \rho_n^2 \omega^2}. \tag{5.165}$$

To assign a physical meaning to the introduced functions $K_1(\omega)$ and $K_2(\omega)$, let us compare the oscillating part of the input strain, that is $-(w_0/h)\cos \omega t$, with the corresponding oscillating part of the compressive stress, which is equal to $-E_3(w_0/h)\left[K_1(\omega)\cos \omega t - K_2(\omega)\sin \omega t\right]$. By analogy with the viscoelastic model, we obtain that $K_1(\omega)$ and $K_2(\omega)$ represent, respectively, the apparent relative storage and loss moduli. Correspondingly, the apparent loss angle, $\delta(\omega)$, can be introduced by the formula

$$\tan \delta(\omega) = \frac{K_2(\omega)}{K_1(\omega)}. \tag{5.166}$$

The apparent loss angle $\delta(\omega)$ describes the phase difference between the displacement input and force output.

In the case of load-controlled compression, following Suh et al. [73], we will assume that the tissue sample is subjected to a cyclic compressive loading

$$F(t) = [F_0(1 - \cos\omega t) + F_1]\mathscr{H}(t), \tag{5.167}$$

where F_0 is the force amplitude, and F_1 is the initial preload.

After substitution of the expression (5.167) into Eq. (5.148), we finally obtain the following resulting strain output:

$$\frac{w(t)}{h} = \frac{1}{\pi a^2 E_3}\left\{F_1 M(t) + F_0\left(\frac{\gamma_1(2-\gamma_0)}{2\gamma_1 - \gamma_2} - \sum_{n=1}^{\infty}\frac{\tau_n^2\omega^2\mathscr{B}_n}{1+\tau_n^2\omega^2}\exp\left(-\frac{t}{\tau_n}\right)\right)\right.$$
$$\left. - F_0\big[M_1(\omega)\cos\omega t + M_2(\omega)\sin\omega t\big]\right\}, \tag{5.168}$$

where we have introduced the notation

$$M_1(\omega) = 1 + \sum_{n=1}^{\infty}\frac{\mathscr{B}_n}{1+\tau_n^2\omega^2}, \tag{5.169}$$

$$M_2(\omega) = \sum_{n=1}^{\infty}\frac{\tau_n\omega\mathscr{B}_n}{1+\tau_n^2\omega^2}. \tag{5.170}$$

Note that $M_1(\omega)$ and $M_2(\omega)$ have physical meanings of the apparent relative storage and loss compliances, respectively.

5.3.7 Displacement-Controlled Unconfined Compression Test

Following Argatov [3], we consider an unconfined compression test with the upper plate displacement specified according to the equation

$$w(t) = w_0 \sin\omega t, \quad t \in (0, \pi/\omega). \tag{5.171}$$

The maximum displacement, w_0, will be achieved at the time moment $t_m = \pi/(2\omega)$. The moment of time $t = \tilde{t}'_M$, when the contact force $F(t)$ vanishes, determines the duration of the contact. The contact force itself can be evaluated according to Eqs. (5.147) and (5.171) as follows:

$$F(t) = \frac{\pi a^2 E_3}{h} w_0 \omega \int_0^t K(t-\tau) \cos \omega\tau \, d\tau. \tag{5.172}$$

According to Eq. (5.172), the contact force at the moment of maximum displacement is given by

$$F(t_m) = \frac{\pi a^2 E_3}{h} w_0 \tilde{K}_1(\omega), \tag{5.173}$$

where we have introduced the notation

$$\tilde{K}_1(\omega) = \omega \int_0^{\pi/(2\omega)} K(\tau) \sin \omega\tau \, d\tau. \tag{5.174}$$

By analogy with the viscoelastic case [2, 4], the quantity $\tilde{K}_1(\omega)$ will be called the reduced incomplete apparent storage modulus.

Substituting the expression (5.143) into the right-hand side of Eq. (5.174), we obtain

$$\tilde{K}_1(\omega) = 1 - \sum_{n=1}^{\infty} \frac{\mathscr{A}_n}{1+\rho_n^2\omega^2} - \sum_{n=1}^{\infty} \frac{\rho_n \omega \mathscr{A}_n}{1+\rho_n^2\omega^2} \exp\Big(-\frac{\pi}{2\omega\rho_n}\Big). \tag{5.175}$$

Now, taking into consideration Eqs. (5.164) and (5.175), we may conclude that the difference between the reduced apparent storage modulus $K_1(\omega)$ and the reduced incomplete apparent storage modulus $\tilde{K}_1(\omega)$ is relatively small at low frequencies. To be more precise, the difference $K_1(\omega) - \tilde{K}_1(\omega)$ is positive and of order $O\big(\omega\rho_1 \exp(-\pi/(2\omega\rho_1))\big)$ as $\omega \to 0$, where ρ_1 is the maximum relaxation time.

In the high frequency limit, the upper limit of the integral (5.174) tends to zero as ω increases. Thus, the behavior of $\tilde{K}_1(\omega)$ as $\omega \to +\infty$ will depend on the behavior of $K(t)$ as $t \to 0$. According to (5.137), as $\omega \to \infty$, we have

$$\tilde{K}_1(\omega) = 1 - \frac{2s_{1/2}}{\sqrt{\pi}} \frac{(\gamma_2 - \gamma_0\gamma_1)}{\gamma_1} \sqrt{\frac{A_{11}^{\mathrm{s}} k_1}{a^2}} \frac{1}{\sqrt{\omega}} + O(\omega^{-1}), \tag{5.176}$$

where $s_{1/2} = \int_0^{\pi/2} \sqrt{x} \sin x \, dx$.

On the other hand, due to the asymptotic formula (5.176), the following limit relation holds true: $\lim K_1(\omega) = 1$ as $\omega \to \infty$. Thus, we conclude that $\tilde{K}_1(\omega) \simeq K_1(\omega)$ for $\omega \to \infty$ as well as $\tilde{K}_1(\omega) \simeq K_1(\omega)$ for $\omega \to 0$. In other words, the reduced incomplete apparent storage modulus $\tilde{K}_1(\omega)$ obeys both asymptotic behaviors of the reduced apparent storage modulus $K_1(\omega)$.

5.3.8 Force-Controlled Unconfined Compression Test

Consider now an unconfined compression test where the external force is as specified by the equation

$$F(t) = F_0 \sin \omega t, \quad t \in (0, \pi/\omega). \tag{5.177}$$

The maximum contact force, F_0, will be achieved at the time moment $t_M = \pi/(2\omega)$. The moment of time $t'_M = \pi/\omega$, when the contact force $F(t)$ vanishes, determines the duration of the compression test. According to Eqs. (5.148) and (5.177), the upper plate displacement can be evaluated as follows:

$$w(t) = \frac{h}{\pi a^2 E_3} F_0 \omega \int_0^t M(t-\tau) \cos \omega\tau \, d\tau. \tag{5.178}$$

Due to Eq. (5.178), the displacement at the moment of maximum contact force is given by

$$w(t_M) = \frac{h}{\pi a^2 E_3} F_0 \tilde{M}_1(\omega), \tag{5.179}$$

where we have introduced the notation

$$\tilde{M}_1(\omega) = \omega \int_0^{\pi/(2\omega)} M(\tau) \sin \omega\tau \, d\tau. \tag{5.180}$$

By analogy with the viscoelastic case [2, 4], the quantity $\tilde{M}_1(\omega)$ will be called the reduced incomplete apparent storage compliance.

Substituting the expression (5.138) into the right-hand side of Eq. (5.180), we obtain

$$\tilde{M}_1(\omega) = 1 + \sum_{n=1}^{\infty} \frac{\mathscr{B}_n}{1+\tau_n^2\omega^2} + \sum_{n=1}^{\infty} \frac{\tau_n \omega \mathscr{B}_n}{1+\tau_n^2\omega^2} \exp\Big(-\frac{\pi}{2\omega\tau_n}\Big). \tag{5.181}$$

Using the same method as for $\tilde{K}_1(\omega)$, it can be shown that the incomplete apparent storage compliance $\tilde{M}_1(\omega)$ obeys both asymptotic behaviors of the apparent storage compliance $M_1(\omega)$, that is $\tilde{M}_1(\omega) \simeq M_1(\omega)$ for $\omega \to 0$ along with $\tilde{M}_1(\omega) \simeq M_1(\omega)$ for $\omega \to \infty$.

5.4 Biphasic Poroviscoelastic (BPVE) Model

In this section, the biphasic poroviscoelastic model is briefly outlined. The confined and unconfined compression tests as well as the torsion test are considered.

5.4.1 Linear Biphasic Poroviscoelastic Theory

The biphasic theory was extended by Mak [54] to account for the inherent viscoelasticity of the solid matrix, by replacing the effective stresses (5.13) in the constitutive equation (5.7) with viscoelastic constitutive relations in the hereditary integral form. Therefore, for a transversely isotropic material, we have

$$\begin{aligned}
\sigma_{11}^{\mathrm{VE}} &= B_{11}^{\mathrm{s}} * \varepsilon_{11} + B_{12}^{\mathrm{s}} * \varepsilon_{22} + B_{13}^{\mathrm{s}} * \varepsilon_{33}, \quad & \sigma_{23}^{\mathrm{VE}} &= 2B_{44}^{\mathrm{s}} * \varepsilon_{23}, \\
\sigma_{22}^{\mathrm{VE}} &= B_{12}^{\mathrm{s}} * \varepsilon_{11} + B_{11}^{\mathrm{s}} * \varepsilon_{22} + B_{13}^{\mathrm{s}} * \varepsilon_{33}, \quad & \sigma_{13}^{\mathrm{VE}} &= 2B_{44}^{\mathrm{s}} * \varepsilon_{13}, \\
\sigma_{33}^{\mathrm{VE}} &= B_{13}^{\mathrm{s}} * \varepsilon_{11} + B_{13}^{\mathrm{s}} * \varepsilon_{22} + B_{33}^{\mathrm{s}} * \varepsilon_{33}, \quad & \sigma_{12}^{\mathrm{VE}} &= 2B_{66}^{\mathrm{s}} * \varepsilon_{12},
\end{aligned} \tag{5.182}$$

where the $*$ sign denotes the Stieltjes integral, i.e.,

$$B_{kl}^{\mathrm{s}} * \varepsilon_{ij} = \int_{-\infty}^{t} B_{kl}^{\mathrm{s}}(t-\tau)\, d\varepsilon_{ij}(\tau). \tag{5.183}$$

For simplicity's sake, following [68], we assume that the deformation behavior of the solid phase is governed by a single reduced stress-relaxation function, $\psi(t)$, which is usually assumed to be in the following form proposed by Fung [28]:

$$\psi(t) = 1 + \int_{0}^{\infty} S(\tau) e^{-t/\tau} d\tau, \tag{5.184}$$

where

$$S(\tau) = \begin{cases} \dfrac{c}{\tau}, & \tau_1 \le \tau \le \tau_2, \\ 0, & \tau < \tau_1, \quad \tau > \tau_2. \end{cases} \tag{5.185}$$

We note (see, e.g., [38, 49]) that the relaxation spectrum (5.185) with constant amplitude over a range of frequencies $\tau \in (\tau_1, \tau_2)$, which was originally introduced by Neubert [61], has least sensitivity to strain rate, which has been believed to be the case for some biological tissues [28].

The function $S(\tau)$ defines a continuous relaxation spectrum, where the parameter c is a proportionality constant for the amplitude of the spectrum $S(\tau)$. The width of the spectrum is defined by the time constants τ_1 and τ_2, which govern the fast and slow relaxation phenomena, respectively.

Note that at initial times after loading and at equilibrium, respectively, we have

$$\psi(0) = 1 + c \ln \frac{\tau_2}{\tau_1}, \quad \psi(+\infty) = 1. \tag{5.186}$$

Therefore, under the above assumptions, the relaxation functions $B^{\mathrm{s}}_{kl}(t)$ can be represented as

$$B^{\mathrm{s}}_{kl}(t) = B^{\mathrm{s}\infty}_{kl}\psi(t), \tag{5.187}$$

where $B^{\mathrm{s}\infty}_{kl} = B^{\mathrm{s}}_{kl}(+\infty)$ are the equilibrium elastic moduli, while the instantaneous elastic moduli, $B^{\mathrm{s}0}_{kl} = B^{\mathrm{s}}_{kl}(0)$, are given by

$$B^{\mathrm{s}0}_{kl} = B^{\mathrm{s}\infty}_{kl}\Big(1 + c\ln\frac{\tau_2}{\tau_1}\Big). \tag{5.188}$$

The viscoelastic parameters c, τ_1, τ_2 are material properties of the solid skeleton that need to be determined from experimental data. The confined and unconfined compression problems for a BPVE material were considered in [34, 36, 54, 68].

Thus, the constitutive equations for the solid matrix in the biphasic poroviscoelastic (BPVE) theory have the form

$$\boldsymbol{\sigma}^{\mathrm{s}} = -\phi_{\mathrm{s}}p\mathbf{I} + \boldsymbol{\sigma}^{\mathrm{VE}}, \tag{5.189}$$

where p is the pressure of the fluid phase, $\mathbf{I}$ is the identity tensor, and the components of the stress tensor $\boldsymbol{\sigma}^{\mathrm{VE}}$ are given by (5.182).

The reduced stress-relaxation function (5.184) and (5.185) can be represented by

$$\psi(t) = 1 + c\Big[E_1\Big(\frac{t}{\tau_2}\Big) - E_1\Big(\frac{t}{\tau_1}\Big)\Big], \tag{5.190}$$

where $E_1(x)$ is the exponential integral function, i.e.,

$$E_1(x) = \int_0^1 \frac{1}{\xi}\exp\Big(-\frac{x}{\xi}\Big)d\xi.$$

Observe [68] that, if the width of the relaxation spectrum reduces to zero, i.e., $\tau_1 \to \tau_2$, the reduced relaxation function (5.190) becomes $\psi(t) = 1$. It is also readily seen that the intrinsic viscoelastic effect diminishes as $c \to 0$. Thus, for the limiting cases $c \to 0$ or $\tau_1 \to \tau_2$, and the BPVE theory reduces to the linear biphasic theory.

Note also that for the sake of numerical efficiency the discrete form of the relaxation function

$$\psi(t) = 1 + \sum_i C_i \exp\Big(-\frac{t}{\tau_i}\Big)$$

has also been used for articular cartilage [21, 72]. Multiple discrete spectrums (different sets of C_i and τ_i) can be used to fit the experimental data for the short-term, mid-term and long-term responses [49].

We finally note [57] that the inclusion of intrinsic matrix viscoelastic properties for the solid matrix in the biphasic theory [54] improved the prediction in the unconfined compression case [68] as well as the material property determination [36, 66].

5.4.2 *Confined Compression of a Biphasic Poroviscoelastic Material*

Under the idealized conditions of the confined compression experiment described in Sect. 5.2.1, the displacement of the solid matrix and the fluid movement occur only in the axial direction, and the governing differential equation (5.63) of the biphasic model should be replaced with the following [54, 68]:

$$\int_{-\infty}^{t} B_{33}^{\mathrm{s}}(t-\tau)\frac{\partial}{\partial\tau}\left(\frac{\partial^2 u_z}{\partial z^2}\right)d\tau = \frac{1}{k_3}\frac{\partial u_z}{\partial t}. \tag{5.191}$$

Here, $u_z(t, z)$ is the axial displacement of the solid phase, k_3 is the axial permeability, and $B_{33}^{\mathrm{s}}(t)$ is the axial aggregate relaxation modulus of the solid phase.

For creep, the initial and boundary conditions are

$$u_z(t, z) = 0, \quad -\infty < t < 0, \tag{5.192}$$

$$\int_{-\infty}^{t} B_{33}^{\mathrm{s}}(t-\tau)\frac{\partial}{\partial\tau}\left(\frac{\partial u_z}{\partial z}\right)d\tau\Bigg|_{z=0} = -\sigma(t)\mathscr{H}(t), \tag{5.193}$$

$$u_z\big|_{z=h} = 0, \tag{5.194}$$

where $\sigma(t)$ is the applied compressive stress (see Eq. (5.63)).

Following [54, 68], we put

$$B_{33}^{\mathrm{s}}(t) = H_A\psi(t), \tag{5.195}$$

where $H_A = B_{33}^{\mathrm{s}\infty}$ is the equilibrium aggregate elastic modulus, and $\psi(t)$ is the reduced stress-relaxation function given by (5.184) and (5.185).

To solve the problem (5.191)–(5.194), we introduce dimensionless quantities

$$\zeta = \frac{z}{h}, \quad \tau = \alpha_1 t, \quad \tau_i' = \alpha_1\tau_i, \quad i = 1, 2, \quad \alpha_1 = \frac{H_A k_3}{h^2} \tag{5.196}$$

and apply the Laplace transform to Eqs. (5.191), (5.193), and (5.194) with respect to the dimensionless time variable τ. In this way, remembering that the Laplace

transform of the function $\psi(\tau/\alpha_1)$ (see Eqs. (5.184) and (5.185)) is given by

$$\tilde{\psi}(s) = \frac{1}{s}\left(1 + c \ln \frac{1 + s\tau_2'}{1 + s\tau_1'}\right), \tag{5.197}$$

we arrive at the problem

$$\begin{aligned} \frac{\partial^2 \tilde{u}_z}{\partial \zeta^2} - f(s)\tilde{u}_z = 0, \qquad \zeta \in (0,1), \\ \frac{\partial \tilde{u}_z}{\partial \zeta}\Big|_{\zeta=0} = -\frac{h}{H_A}\frac{f(s)\tilde{\sigma}(s)}{s}, \quad \tilde{u}_z\big|_{\zeta=1} = 0, \end{aligned} \tag{5.198}$$

where we have introduced the notation

$$f(s) = \frac{1}{\tilde{\psi}(s)}. \tag{5.199}$$

From (5.198), we readily obtain

$$\tilde{u}_z = \frac{h\tilde{\sigma}(s)\sqrt{f(s)}}{H_A s}\frac{\sinh\left[\sqrt{f(s)}(1-\zeta)\right]}{\cosh\sqrt{f(s)}}. \tag{5.200}$$

In the case where a constant external load, F_0, is applied instantaneously, we have $\sigma(t) = \sigma_0 \mathscr{H}(t)$, where $\sigma_0 = F_0/A$ with A being the sample cross-sectional area, and $\tilde{\sigma}(s) = \sigma_0/s$, so that formula (5.200) reduces to the fallowing [54, 68]:

$$\tilde{u}_z = \frac{h\sigma_0}{H_A}\frac{\sqrt{f(s)}\sinh\left[\sqrt{f(s)}(1-\zeta)\right]}{s^2\cosh\sqrt{f(s)}}.$$

An asymptotic approximation of the surface displacement $u_z|_{z=0}$ for small times after loading can be obtained by evaluating the inverse Laplace transform as $s \to \infty$, when $f(s) \sim s/\alpha_2$, for a constant α_2. Taking into account (5.197), (5.199) and the relation $\tau_2'/\tau_1' = \tau_2/\tau_1$ (see Eq. $(5.196)_3$), we get

$$\alpha_2 = 1 + c \ln \frac{\tau_2}{\tau_1}.$$

Thus, the short-time asymptotic approximation for the nominal sample-average strain is given by the following formula [54, 68]:

$$\frac{u_z(t,0)}{h} \simeq \frac{2\sigma_0}{H_A}\sqrt{\frac{\alpha_1}{\pi\alpha_2}}t.$$

Note that $\alpha_2 = \psi(0)$ (see Eqs. (5.184) and (5.185)). This dimensionless parameter characterizes the intrinsic solid matrix viscoelastic effects. Observe also [68] that

larger values of α_2, reflecting increased effects of matrix viscoelasticity, or lower values of α_1, and reflecting a low value of the solid matrix permeability, will have the same effect in reducing the early creep response.

5.4.3 Unconfined Compression of a BPVE Material

In the framework of the BPVE theory, the unconfined compression problem (considered previously in Sect. 5.3.1) differs in essence via the constitutive equations (5.98), which now take the form

$$\begin{aligned}
\sigma_{rr}^{\mathrm{VE}} &= B_{11}^{\mathrm{s}} * \frac{\partial u_r}{\partial r} + B_{12}^{\mathrm{s}} * \frac{u_r}{r} + B_{13}^{\mathrm{s}} * \varepsilon, \\
\sigma_{\theta\theta}^{\mathrm{VE}} &= B_{12}^{\mathrm{s}} * \frac{\partial u_r}{\partial r} + B_{11}^{\mathrm{s}} * \frac{u_r}{r} + B_{13}^{\mathrm{s}} * \varepsilon, \\
\sigma_{zz}^{\mathrm{VE}} &= B_{13}^{\mathrm{s}} * \frac{\partial u_r}{\partial r} + B_{13}^{\mathrm{s}} * \frac{u_r}{r} + B_{33}^{\mathrm{s}} * \varepsilon.
\end{aligned} \tag{5.201}$$

The equilibrium equation of the solid matrix (5.99) now has the form

$$-\frac{\partial p}{\partial r} + B_{11}^{\mathrm{s}} * \left(\frac{\partial^2 u_r}{\partial r^2} + \frac{1}{r}\frac{\partial u_r}{\partial r} - \frac{u_r}{r^2} \right) = 0.$$

We recall that the boundary conditions (5.91)–(5.93) are formulated in terms of the components of the total stress tensor

$$\boldsymbol{\sigma} = -p\mathbf{I} + \boldsymbol{\sigma}^{\mathrm{VE}}. \tag{5.202}$$

To solve this problem, let us first introduce the dimensionless variables

$$\rho = \frac{r}{a}, \quad U = \frac{u_r}{a},$$

where we have refrained from using the variables t and p in the non-dimensionalization. Secondly, we apply the Laplace transform with respect to the time variable t, denoting by a tilde the transformed quantities. We then introduce auxiliary notation

$$\tilde{P} = \frac{\tilde{p}}{\bar{B}_{11}^{\mathrm{s}}(s)}, \quad \alpha_{12} = \frac{\bar{B}_{12}^{\mathrm{s}}(s)}{\bar{B}_{11}^{\mathrm{s}}(s)}, \quad \alpha_{13} = \frac{\bar{B}_{13}^{\mathrm{s}}(s)}{\bar{B}_{11}^{\mathrm{s}}(s)}, \quad \alpha_{33} = \frac{\bar{B}_{33}^{\mathrm{s}}(s)}{\bar{B}_{11}^{\mathrm{s}}(s)}, \tag{5.203}$$

$$f(s) = \frac{a^2 s}{k_1 \bar{B}_{11}^{\mathrm{s}}(s)}, \quad \bar{B}_{kl}^{\mathrm{s}}(s) = s\tilde{B}_{kl}^{\mathrm{s}}(s). \tag{5.204}$$

In this case, the biphasic unconfined compression problem (5.111)–(5.113) is replaced with the following:

$$\frac{\partial \tilde{P}}{\partial \rho} = f(s)\Big(\tilde{U} + \frac{\tilde{\varepsilon}}{2}\rho\Big),$$

$$\frac{\partial^2 \tilde{U}}{\partial \rho^2} + \frac{1}{\rho}\frac{\partial \tilde{U}}{\partial \rho} - \frac{\tilde{U}}{\rho^2} = f(s)\Big(\tilde{U} + \frac{\tilde{\varepsilon}}{2}\rho\Big),$$

$$\tilde{P}\big|_{\rho=1} = 0, \quad \frac{\partial \tilde{U}}{\partial \rho} + \alpha_{12}(s)\frac{\tilde{U}}{\rho} + \alpha_{13}(s)\tilde{\varepsilon}\,\Big|_{\rho=1} = 0.$$

In the same way as was done in Sect. 5.3.2, we find

$$\tilde{U} = -\frac{\tilde{\varepsilon}(s)}{2}\rho\left(1 - \frac{(1+\alpha_{12}(s)-2\alpha_{13}(s))\dfrac{I_1(\sqrt{f(s)}\rho)}{\sqrt{f(s)}\rho}}{I_0(\sqrt{f(s)}) - (1-\alpha_{12}(s))\dfrac{I_1(\sqrt{f(s)})}{\sqrt{f(s)}}}\right), \tag{5.205}$$

$$\tilde{p} = \frac{(1+\alpha_{12}(s)-2\alpha_{13}(s))\tilde{\varepsilon}(s)\big[I_0(\sqrt{f(s)}\rho) - I_0(\sqrt{f(s)})\big]}{2\left(I_0(\sqrt{f(s)}) - (1-\alpha_{12}(s))\dfrac{I_1(\sqrt{f(s)})}{\sqrt{f(s)}}\right)}. \tag{5.206}$$

We now consider the force response of the BPVE sample

$$F(t) = -2\pi\int_0^a \sigma_{zz}(t,r)r\,dr, \tag{5.207}$$

where, as a result of (5.201) and (5.202), the normal total stress is given by

$$\sigma_{zz}(t,r) = -p + B_{13}^{\mathrm{s}} * \left(\frac{\partial u_r}{\partial r} + \frac{u_r}{r}\right) + B_{33}^{\mathrm{s}} * \varepsilon.$$

Upon application of the Laplace transform to Eq. (5.207), rewritten in terms of the dimensionless variables (5.203), we obtain

$$\frac{\tilde{F}(s)}{\pi a^2 \bar{B}_{11}^{\mathrm{s}}(s)} = -2\int_0^1 \left(-\tilde{P} + \alpha_{13}(s)\Big(\frac{\partial \tilde{U}}{\partial \rho} + \frac{\tilde{U}}{\rho}\Big) + \alpha_{33}(s)\tilde{\varepsilon}\right)\rho\,d\rho.$$

Taking into account formulas (5.205) and (5.206), and performing the integration in the above equation, we arrive at formula (5.126), where the coefficients γ_0, γ_1, and γ_2 are evaluated by Eq. (5.127), where α_{12}, α_{13}, and α_{33} are as given by (5.203).

Finally, note that the instantaneous axial modulus E_3, in light of (5.149), is

$$E_3 = \frac{1}{2}\left(B_{11}^{s0} + B_{12}^{s0} + 2B_{33}^{s0} - 4B_{13}^{s0}\right),$$

where $B_{kl}^{s0} = B_{kl}^{s}(0)$ are the instantaneous elastic moduli of the solid matrix.

We can thus hypothesize that the instantaneous response of a transversely isotropic biphasic poroviscoelastic tissue is equivalent to that of an incompressible transversely isotropic elastic material with the material constants given by formulas (5.36), (5.39), and (5.40), where ν_{12}^{s}, ν_{31}^{s}, G_{13}^{s}, E_1^{s}, and E_3^{s} are regarded as instantaneous elastic material properties of the poroviscoelastic matrix.

Observe that the deformation response of a biphasic or BPVE sample depends on how it is tested. In particular, while only the aggregate relaxation modulus $B_{33}^{s}(t)$ governs the behavior of a sample tested in confined compression, all four relaxation moduli $B_{11}^{s}(t)$, $B_{12}^{s}(t)$, $B_{13}^{s}(t)$, and $B_{33}^{s}(t)$ have significant influence on the deformation behavior of a BPVE sample tested in unconfined compression.

Finally, we note [34] that the failure to account for either anisotropy or viscoelasticity of the articular cartilage matrix could result in flawed predictions of the tissue deformation under general external loading.

5.4.4 Torsion of a Biphasic Poroviscoelastic Material

We consider a cylindrical sample of a BPVE material of radius a and height h subjected to a torque T (see Fig. 5.7). Let θ denotes the angle of torsional displacement imposed on the upper surface of the sample to achieve a specified shear strain, γ. Between these geometrical parameters, the following relation takes place:

$$\gamma = \vartheta a. \tag{5.208}$$

Here, $\vartheta = \theta/h$ is the so-called twist, defined as the angle of rotation per unit length along the axis of the sample.

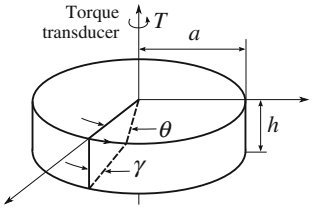

Fig. 5.7 Schematic of the pure torsional shear testing configuration

The components of the in-plane displacement vector are $u_r = 0$ and $u_\theta = \vartheta r z$, and so the only nonzero component of strain is

$$\varepsilon_{z\theta} = \frac{1}{2}\vartheta r. \tag{5.209}$$

The torque is given by

$$T = 2\pi \int_0^a r^2 \sigma_{z\theta}\, dr, \tag{5.210}$$

where according to (5.182) and (5.202) the total shear stress $\sigma_{z\theta}$ is related to the shear strain component $\varepsilon_{z\theta}$ as follows:

$$\sigma_{z\theta} = 2 \int_{-\infty}^{t} B_{44}^{\mathrm{s}}(t-\tau) \frac{\partial \varepsilon_{z\theta}}{\partial \tau}(\tau)\, d\tau. \tag{5.211}$$

Therefore, the substitution of (5.209) and (5.211) into Eq. (5.210) yields

$$T(t) = I_{\mathrm{p}} \int_{-\infty}^{t} B_{44}^{\mathrm{s}}(t-\tau) \frac{\partial \vartheta}{\partial \tau}(\tau)\, d\tau, \tag{5.212}$$

where $I_{\mathrm{p}} = \pi a^4/2$ is the polar moment of inertia of the sample's cross section area.

Furthermore, introducing the so-called shear stress

$$\tau = \frac{aT}{I_{\mathrm{p}}},$$

which is defined as maximum shear stress in the sample, and taking into account (5.208), we can rewrite Eq. (5.212) in terms of the shear strain as follows:

$$\tau(t) = \int_{-\infty}^{t} B_{44}^{\mathrm{s}}(t-t') \frac{\partial \gamma}{\partial t'}(t')\, dt'. \tag{5.213}$$

Now, assuming that the employed herein viscoelastic material of the solid phase is described by the Fung model [28], we represent the above equation in the form

$$\tau(t) = B_{44}^{\mathrm{s}\infty} \int_{-\infty}^{t} \psi(t-t') \frac{\partial \gamma}{\partial t'}(t')\, dt', \tag{5.214}$$

where $B_{44}^{s\infty}$ is the equilibrium out-of-plane shear modulus, and $\psi(t)$ is the reduced relaxation function given by (5.184) and (5.185), i.e.,

$$\psi(t) = 1 + c \int_{\tau_1}^{\tau_2} \frac{1}{\tau} \exp\Big(-\frac{t}{\tau}\Big) d\tau. \tag{5.215}$$

Following Iatridis et al. [38], we now outline the main shear testing protocols.

Stress-relaxation behavior. In the stress-relaxation experiments, the sample is subjected to a ramping phase, where the strain increases linearly at a constant strain rate, followed by a relaxation phase, where the shear strain is held constant, i.e.,

$$\gamma(t) = \begin{cases} \dfrac{\gamma_0}{t_0} t, & 0 \le t \le t_0, \\ \gamma_0, & t_0 \le t, \end{cases}$$

where γ_0 and t_0 are given constants.

For the ramping phase ($0 \le t \le t_0$), we have

$$\tau(t) = \frac{B_{44}^{s\infty}\gamma_0}{t_0}\big[t + c_1 F_1(t, \tau_1, \tau_2)\big],$$

where (with $E_i(x)$ being the exponential integral)

$$F_1(t, \tau_1, \tau_2) = \tau_2\big(1 - e^{-t/\tau_2}\big) - \tau_1\big(1 - e^{-t/\tau_1}\big) - t\big[E_i(t/\tau_1) - E_i(t/\tau_2)\big],$$

$$E_i(x) = \int_x^{\infty} \frac{\exp(-\xi)}{\xi}\, d\xi.$$

For the stress-relaxation phase, the solution is given in terms of the shifted time parameter $\hat{t} = t - t_0$ in the following form [38]:

$$\tau(t) = \frac{B_{44}^{s\infty}\gamma_0}{t_0}\big[t_0 + c_1 G_1(t, \hat{t}, \tau_1, \tau_2)\big],$$

where

$$\begin{aligned} G_1(t, \hat{t}, \tau_1, \tau_2) = {} & \tau_2\big(e^{-\hat{t}/\tau_2} - e^{-t/\tau_2}\big) - \tau_1\big(e^{-\hat{t}/\tau_1} - e^{-t/\tau_1}\big) \\ & - \big\{\hat{t}\big[E_i(\hat{t}/\tau_2) - E_i(\hat{t}/\tau_1)\big] - t\big[E_i(t/\tau_2) - E_i(t/\tau_1)\big]\big\}. \end{aligned}$$

Creep behavior. Let us introduce the out-of-plane creep compliance in shear of the solid matrix, $J_{44}^{s}(t)$, which governs the deformation response of the solid phase under application of a step out-of-plane shear stress of unit magnitude. Hence, the

inverse relation for (5.213) is given by

$$\gamma(t) = \int_{0^-}^{t} J_{44}^{\mathrm{s}}(t-t')\frac{\partial \tau}{\partial t'}(t')\,dt'. \tag{5.216}$$

For a given relaxation modulus $B_{44}^{\mathrm{s}}(t)$, the corresponding creep compliance can be evaluated via its Laplace transform

$$\tilde{J}_{44}^{\mathrm{s}}(s) = \frac{1}{s^2\tilde{B}_{44}^{\mathrm{s}}(s)}. \tag{5.217}$$

Let us now introduce the reduced creep function, $\varphi(t)$, by the formula

$$J_{44}^{\mathrm{s}}(t) = J_{44}^{\mathrm{s}\infty}\varphi(t), \tag{5.218}$$

where $J_{44}^{\mathrm{s}\infty} = J_{44}^{\mathrm{s}}(+\infty)$ is the equilibrium compliance. Since the reduced stress-relaxation function is defined by $\psi(t) = B_{44}^{\mathrm{s}}(t)/B_{44}^{\mathrm{s}\infty}$, where $B_{44}^{\mathrm{s}\infty}$ is the equilibrium modulus such that $B_{44}^{\mathrm{s}\infty} = 1/J_{44}^{\mathrm{s}\infty}$, the following normalization conditions hold:

$$\psi(+\infty) = 1, \quad \varphi(+\infty) = 1.$$

The Fung reduced creep function $\varphi(t)$ corresponding to the reduced relaxation function $\psi(t)$ given by Eq. (5.218) can be obtained by employment of the Laplace transform and Eq. (5.217), that is

$$\tilde{\psi}(s)\tilde{\varphi}(s) = \frac{1}{s^2},$$

where the Laplace transform $\tilde{\psi}(s)$ is given by formula (5.197).

According to Dortmans et al. [22], the following formula holds:

$$\begin{aligned}\varphi(t) = 1 &- \frac{(\tau_c-\tau_2)(\tau_c-\tau_1)}{c\tau_c(\tau_2-\tau_1)}e^{-t/\tau_c} \\ &- c\int_{\tau_1}^{\tau_2} e^{-t/\tau}\frac{1}{\tau}\frac{1}{\left(1+c\ln\dfrac{\tau_2-\tau}{\tau-\tau_1}\right)^2+\pi^2c^2}\,d\tau,\end{aligned} \tag{5.219}$$

where we have used the notation

$$\tau_c = \frac{\tau_2 e^{1/c}-\tau_1}{e^{1/c}-1}.$$

In the creep experiment, a constant torque, T_0, is applied instantaneously, i.e., $T(t) = T_0\mathscr{H}(t)$ and $\tau(t) = \tau_0\mathscr{H}(t)$, where $\tau_0 = aT_0/I_\mathrm{p}$. Therefore, by formulas (5.216) and (5.218), we obtain

$$\gamma(t) = \tau_0 J_{44}^{\mathrm{s}\infty}\varphi(t),$$

where $\varphi(t)$ is given by (5.219).

Steady sinusoidal behavior. If the sample is subjected to a dynamic frequency sweep, the sinusoidal shear strain input is given by

$$\gamma = \gamma_0 e^{\mathrm{i}\omega t},$$

where γ_0 (rad) is the peak shear strain, ω (rad/s) is the angular frequency, and i is the imaginary unit equal to the square root of -1.

In the absence of inertial forces, the corresponding shear stress output will be

$$\tau = \tau_0 e^{\mathrm{i}\omega t},$$

where τ_0 is a complex quantity.

The ratio of the amplitudes τ_0 and γ_0 determines the reduced complex elastic shear modulus, ψ^*, such that

$$\tau_0 = B_{44}^{\mathrm{s}\infty}\psi^*\gamma_0.$$

The reduced complex modulus ψ^* is comprised of real and imaginary parts, i.e.,

$$\psi^* = \psi_1 + \mathrm{i}\psi_2,$$

which defines as the reduced storage, ψ_1, and loss, ψ_2, modulus, respectively.

The reduced storage and loss moduli as functions of angular frequency are evaluated as follows [38]:

$$\psi_1(\omega) = 1 + \frac{c}{2}\ln\frac{1+(\omega\tau_2)^2}{1+(\omega\tau_1)^2},$$

$$\psi_2(\omega) = c\left\{\tan^{-1}(\omega\tau_2) - \tan^{-1}(\omega\tau_1)\right\}.$$

The torsional shear configuration shown in Fig. 5.7 has been used to study equilibrium and dynamic shear moduli as well as the characterization of the stress-relaxation behavior of articular cartilage. Note also [15] that other types of shear testing (for instance, single-lap test) may be important in determining the capacity of cartilage to repair.

It is also noteworthy that under a small shear strain no volumetric changes or pressure gradients occur in a cylindrical sample of BPVE material, and therefore no interstitial fluid flow is induced. Thus, shear tests under infinitesimal strain enable

evaluation of the intrinsic viscoelastic, flow-independent properties of the collagen-proteoglycan solid matrix [18, 41].

Finally, we note that a finite element formulation for describing the large deformation response of biphasic materials in torsion was presented in [56], with a specific focus on the consideration of nonlinear coupling between torsional deformation and fluid pressurization in articular cartilage.

References

1. Appleyard, R.C., Swain, M.V., Khanna, S., Murrell, G.A.C.: The accuracy and reliability of a novel handheld dynamic indentation probe for analysing articular cartilage. Phys. Med. Biol. **46**, 541–550 (2001)
2. Argatov, I.: Sinusoidally-driven flat-ended indentation of time-dependent materials: Asymptotic models for low and high rate loading. Mech. Mater. **48**, 56–70 (2012)
3. Argatov, I.: Sinusoidally-driven unconfined compression test for a biphasic tissue. arXiv preprint arXiv:1207.4679 (2012)
4. Argatov, I., Daniels, A.U., Mishuris, G., Ronken, S., Wirz, D.: Accounting for the thickness effect in dynamic spherical indentation of a viscoelastic layer: application to non-destructive testing of articular cartilage. Eur. J. Mech. A/Solids **37**, 304–317 (2013)
5. Armstrong, C.G., Lai, W.M., Mow, V.C.: An analysis of the unconfined compression of articular cartilage. J. Biomech. Eng. **106**, 165–173 (1984)
6. Ateshian, G.A., Ellis, B.J., Weiss, J.A.: Equivalence between short-time biphasic and incompressible elastic material responses. J. Biomech. Eng. **129**, 405–412 (2007)
7. Ateshian, G.A., Lai, W.M., Zhu, W.B., Mow, V.C.: An asymptotic solution for the contact of two biphasic cartilage layers. J. Biomech. **27**, 1347–1360 (1994)
8. Ateshian, G.A., Warden, W.H., Kim, J.J., Grelsamer, R.P., Mow, V.C.: Finite deformation biphasic material properties of bovine articular cartilage from confined compression experiments. J. Biomech. **30**, 1157–1164 (1997)
9. Barry, S.I., Aldis, G.K.: Comparison of models for flow induced deformation of soft biological tissue. J. Biomech. **23**, 647–654 (1990)
10. Barry, S.I., Holmes, M.: Asymptotic behaviour of thin poroelastic layers. IMA J. Appl. Math. **66**, 175–194 (2001)
11. Barry, S.I., Mercer, G.N.: Flow and deformation in poroelasticity—i unusual exact solutions. Math. Comp. Model. **30**, 23–29 (1999)
12. Biot, M.A.: Theory of finite deformations of porous solids. Indiana Univ. Math. J. **21**, 597–620 (1972)
13. Boschetti, F., Pennati, G., Gervaso, F., Peretti, G.M., Dubini, G.: Biomechanical properties of human articular cartilage under compressive loads. Biorheology **41**, 159–166 (2004)
14. Buschmann, M.D.: Numerical conversion of transient to harmonic response functions for linear viscoelastic materials. J. Biomech. **30**, 197–202 (1997)
15. Chen, A.C., Klisch, S.M., Bae, W.C., Temple, M.M., McGowan, K.B., Gratz, K.R., Schumacher, B.L., Sah, R.L.: Mechanical characterization of native and tissue-engineered cartilage. In: de Ceuninck, F., Sabatini, M., Pastoureau, Ph (eds.) Cartilage and Osteoarthritis, pp. 157–190. Humana Press, Totowa, NJ (2004)
16. Chen, X., Dunn, A.C., Sawyer, W.G., Sarntinoranont, M.: A biphasic model for micro-indentation of a hydrogel-based contact lens. J. Biomech. Eng. **129**, 156–163 (2007)
17. Chin, H.C., Khayat, G., Quinn, T.M.: Improved characterization of cartilage mechanical properties using a combination of stress relaxation and creep. J. Biomech. **44**, 198–201 (2011)
18. Cohen, N.P., Foster, R.J., Mow, V.C.: Composition and dynamics of articular cartilage: structure, function, and maintaining healthy state. J. Orthop. Sports Phys. Ther. **28**, 203–215 (1998)

19. Cohen, B., Lai, W.M., Mow, V.C.: A transversely isotropic biphasic model for unconfined compression of growth plate and chondroepiphysis. J. Biomech. Eng. **120**, 491–496 (1998)
20. Cowin, S.C.: Bone poroelasticity. J. Biomech. **32**, 217–238 (1999)
21. DiSilvestro, M.R., Suh, J.-K.F.: A cross-validation of the biphasic poroviscoelastic model of articular cartilage in unconfined compression, indentation, and confined compression. J. Biomech. **34**, 519–525 (2001)
22. Dortmans, L.J.M.G., van de Ven, A.A.F., Sauren, A.A.H.J.: A note on the reduced creep function corresponding to the quasi-linear visco-elastic model proposed by Fung. J. Biomech. Eng. **116**, 373–375 (1994)
23. Eberhardt, A.W., Keer, L.M., Lewis, J.L., Vithoontien, V.: An analytical model of joint contact. J. Biomech. Eng. **112**, 407–413 (1990)
24. Ehlers, W., Markert, B.: On the viscoelastic behaviour of fluid-saturated porous materials. Granular Matter **2**, 153–161 (2000)
25. Federico, S., Herzog, W.: On the anisotropy and inhomogeneity of permeability in articular cartilage. Biomech. Model. Mechanobiol. **7**, 367–378 (2008)
26. Federico, S., Grillo, A., Giaquinta, G., Herzog, W.: A semi-analytical solution for the confined compression of hydrated soft tissue. Meccanica **44**, 197–205 (2009)
27. Freutel, M., Schmidt, H., Dürselen, L., Ignatius, A., Galbusera, F.: Finite element modeling of soft tissues: material models, tissue interaction and challenges. Clin. Biomech. **29**, 363–372 (2014)
28. Fung, Y.C.: Biomechanics: Mechanical Properties of Living Tissues. Springer-Verlag, New York (1981)
29. Garcia, J.J., Altiero, N.J., Haut, R.C.: An approach for the stress analysis of transversely isotropic biphasic cartilage under impact load. J. Biomech. Eng. **120**, 608–613 (1998)
30. Gradshteyn, I.S., Ryzhik, I.M.: Table of Integrals, Series, and Products. Academic, New York (1980)
31. Gu, W.Y., Lai, W.M., Mow, V.C.: A mixture theory for charged hydrated soft tissues containing multi-electrolytes: passive transport and swelling behaviors. J. Biomech. Eng. **120**, 169–180 (1998)
32. Hatami-Marbini, H., Etebu, E.: An experimental and theoretical analysis of unconfined compression of corneal stroma. J. Biomech. **46**, 1752–1758 (2013)
33. Higginson, G.R., Litchfield, M.R., Snaith, J.: Load-deformation-time characteristics of articular cartilage. Int. J. mech. Sci. **18**, 481–486 (1976)
34. Hoang, S.K., Abousleiman, Y.N.: Poroviscoelasticity of transversely isotropic cylinders under laboratory loading conditions. Mech. Res. Commun. **37**, 298–306 (2010)
35. Hou, J.S., Mow, V.C., Lai, W.M., Holmes, M.H.: An analysis of the squeeze-film lubrication mechanism for articular cartilage. J. Biomech. **25**, 247–259 (1992)
36. Huang, C.-Y., Mow, V.C., Ateshian, G.A.: The role of flow-independent viscoelasticity in the biphasic tensile and compressive responses of articular cartilage. J. Biomech. Eng. **123**, 410–417 (2001)
37. Huyghe, J.M., Janssen, J.D.: Quadriphasic mechanics of swelling incompressible porous media. Int. J. Eng. Sci. **35**, 793–802 (1997)
38. Iatridis, J.C., Setton, L.A., Weidenbaum, M., Mow, V.C.: The viscoelastic behavior of the non-degenerate human lumbar nucleus pulposus in shear. J. Biomech. **30**, 1005–1013 (1997)
39. Itskov, M., Aksel, N.: Elastic constants and their admissible values for incompressible and slightly compressible anisotropic materials. Acta Mech. **157**, 81–96 (2002)
40. Johnson, M., Tarbell, J.M.: A biphasic, anisotropic model of the aortic wall. J. Biomech. Eng. **123**, 52–57 (2000)
41. Knecht, S., Vanwanseele, B., Stüssi, E.: A review on the mechanical quality of articular cartilage—Implications for the diagnosis of osteoarthritis. Clin. Biomech. **21**, 999–1012 (2006)
42. Kluge, J.A., Rosiello, N.C., Leisk, G.G., Kaplan, D.L., Dorfmann, A.L.: The consolidation behavior of silk hydrogels. J. Mech. Behav. Biomed. Mater. **3**, 278–289 (2010)
43. Korhonen, R.K., Laasanen, M.S.: Töyräs, J., Rieppo, J., Hirvonen, J., Helminen, H.J., Jurvelin, J.S.: Comparison of the equilibrium response of articular cartilage in unconfined compression, confined compression and indentation. J. Biomech. **35**, 903–909 (2002)

44. Lai, W.M., Mow, V.C.: Drug-induced compression of articular cartilage during a permeation experiment. Biorheology **17**, 111–123 (1980)
45. Lai, W.M., Hou, J.S., Mow, V.C.: A triphasic theory for the swelling and deformational behaviors of articular cartilage. J. Biomech. Eng. **113**, 245–258 (1991)
46. Lavrentyev, M.A., Shabat, B.V.: Methods of Complex Variable Functions. Nauka, Moscow (1987) (in Russian)
47. Leipzig, N.D., Athanasiou, K.A.: Unconfined creep compression of chondrocytes. J. Biomech. **38**, 77–85 (2005)
48. LePage, W.R.: Complex Variables and the Laplace Transform for Engineers. McGraw-Hill, New York (1961)
49. Li, L.P., Ahsanizadeh, S.: Computational modelling of articular cartilage. In: Jin, Z. (ed.) Computational Modelling of Biomechanics and Biotribology in the Musculoskeletal System: Biomaterials and Tissues, pp. 205–243. Woodhead Publications, Cambridge (2014)
50. Li, L.P., Korhonen, R.K., Iivarinen, J., Jurvelin, J.S., Herzog, W.: Fluid pressure driven fibril reinforcement in creep and relaxation tests of articular cartilage. Med. Eng. Phys. **30**, 182–189 (2008)
51. Li, S., Patwardhan, A.G., Amirouche, F.M.L., Havey, R., Meade, K.P.: Limitations of the standard linear solid model of intervertebral discs subject to prolonged loading and low-frequency vibration in axial compression. J. Biomech. **28**, 779–790 (1995)
52. Lu, X.L., Mow, V.C.: Biomechanics of articular cartilage and determination of material properties. Med. Sci. Sports Exerc. **40**, 193–199 (2008)
53. Lu, X.L., Miller, C., Chen, F.H., Guo, X.E., Mow, V.C.: The generalized triphasic correspondence principle for simultaneous determination of the mechanical properties and proteoglycan content of articular cartilage by indentation. J. Biomech. **40**, 2434–2441 (2006)
54. Mak, A.F.: The apparent viscoelastic behavior of articular cartilage—the contributions from the intrinsic matrix viscoelasticity and interstitial fluid flows. J. Biomech. Eng. **108**, 123–130 (1986)
55. Markert, B.: A constitutive approach to 3-d nonlinear fluid flow through finite deformable porous continua. Transport Porous Med. **70**, 427–450 (2007)
56. Meng, X.N., LeRoux, M.A., Laursen, T.A., Setton, L.A.: A nonlinear finite element formulation for axisymmetric torsion of biphasic materials. Int. J. Solids Struct. **39**, 879–895 (2002)
57. Mow, V.C., Guo, X.E.: Mechano-electrochemical properties of articular cartilage: their inhomogeneities and anisotropies. Annu. Rev. Biomed. Eng. **4**, 175–209 (2002)
58. Mow, V.C., Lai, W.M.: Recent developments in synovial joint biomechanics. SIAM Rev. **22**, 275–317 (1980)
59. Mow, V.C., Holmes, M.H., Lai, W.M.: Fluid transport and mechanical properties of articular cartilage: a review. J. Biomech. **17**, 377–394 (1984)
60. Mow, V.C., Kuei, S.C., Lai, W.M., Armstrong, C.G.: Biphasic creep and stress relaxation of articular cartilage in compression: theory and experiments. J. Biomech. Eng. **102**, 73–84 (1980)
61. Neubert, H.K.P.: A simple model representing internal damping in solid materials. Aeronaut. Quart. **14**, 187–210 (1963)
62. Oomens, C.W.J., Van Campen, D.H., Grootenboer, H.J.: A mixture approach to the mechanics of skin. J. Biomech. **20**, 877–885 (1987)
63. Park, S., Krishnan, R., Nicoll, S.B., Ateshian, G.A.: Cartilage interstitial fluid load support in unconfined compression. J. Biomech. **36**, 1785–1796 (2003)
64. Polyanin, A.D.: Handbook of Linear Partial Differential Equations for Engineers and Scientists. Chapman and Hall/CRC Press, Boca Raton, London (2002)
65. Peña, E., Del Palomar, A.P., Calvo, B., Martínez, M.A., Doblaré, M.: Computational modelling of diarthrodial joints. Physiological, pathological and pos-surgery simulations. Arch. Comput. Methods. Eng. **14**, 47–91 (2007)
66. Raghunathan, S., Evans, D., Sparks, J.L.: Poroviscoelastic modeling of liver biomechanical response in unconfined compression. Ann. Biomed. Eng. **38**, 1789–1800 (2010)
67. Reynaud, B., Quinn, T.M.: Anisotropic hydraulic permeability in compressed articular cartilage. J. Biomech. **39**, 131–137 (2006)

68. Setton, L.A., Zhu, W., Mow, V.C.: The biphasic poroviscoelastic model for articular cartilage: theory and experiment. J. Biomech. **26**, 581–592 (1993)
69. Soltz, M.A., Ateshian, G.A.: Experimental verification and theoretical prediction of interstitial fluid pressurization at an impermeable contact interface in confined compression. J. Biomech. **31**, 927–934 (1998)
70. Soltz, M.A., Ateshian, G.A.: Interstitial fluid pressurization during confined compression cyclical loading of articular cartilage. Ann. Biomed. Eng. **28**, 150–159 (2000)
71. Spilker, R.L., Suh, J.K., Mow, V.C.: Effects of friction on the unconfined compressive response of articular cartilage: a finite element analysis. J. Biomech. Eng. **112**, 138–146 (1990)
72. Suh, J.-K., Bai, S.: Finite element formulation of biphasic poroviscoelastic model for articular cartilage. J. Biomech. Eng. **120**, 195–201 (1998)
73. Suh, J.-K., Li, Z., Woo, S.L.-Y.: Dynamic behavior of a biphasic cartilage model under cyclic compressive loading. J. Biomech. **28**, 357–364 (1995)
74. Terzaghi, K.: Theoretical Soil Mechanics. Wiley, New York (1942)
75. Wang, C.C.-B., Hung, C.T., Mow, V.C.: An analysis of the effects of depth-dependent aggregate modulus on articular cartilage stress-relaxation behavior in compression. J. Biomech. **34**, 75–84 (2001)
76. Wilson, W., Van Donkelaar, C.C., Van Rietbergen, R., Huiskes, R.: The role of computational models in the search for the mechanical behavior and damage mechanisms of articular cartilage. Med. Eng. Phys. **27**, 810–826 (2005)
77. Wu, J.Z., Dong, R.G., Schopper, A.W.: Analysis of effects of friction on the deformation behavior of soft tissues in unconfined compression tests. J. Biomech. **37**, 147–155 (2004)